Developmental Biology 476 (2021) 53–67

Contents lists available at ScienceDirect

Developmental Biology

journal homepage: www.elsevier.com/locate/developmentalbiology

CREB-binding protein (CBP) gene family regulates planarian survival and stem cell differentiation

Susanna Fraguas [a,b], Sheila Cárcel [a,1], Coral Vivancos [a,1], Ma Dolores Molina [a,b], Jordi Ginés [a], Judith Mazariegos [a], Thileepan Sekaran [d], Kerstin Bartscherer [c], Rafael Romero [a], Francesc Cebrià [a,b,*]

[a] Department of Genetics, Microbiology and Statistics, Faculty of Biology, University of Barcelona, Spain
[b] Institute of Biomedicine of the University of Barcelona (IBUB), Spain
[c] Hubrecht Institute, the Netherlands
[d] EMBL, Heidelberg, Germany

ARTICLE INFO

Keywords:
Planaria
Differentiation
Regeneration
Stem cells
CBP/p300 proteins

ABSTRACT

In developmental biology, the regulation of stem cell plasticity and differentiation remains an open question. CBP(CREB-binding protein)/p300 is a conserved gene family that functions as a transcriptional co-activator and plays important roles in a wide range of cellular processes, including cell death, the DNA damage response, and tumorigenesis. The acetyl transferase activity of CBPs is particularly important, as histone and non-histone acetylation results in changes in chromatin architecture and protein activity that affect gene expression. Many studies have described the conserved functions of CBP/p300 in stem cell proliferation and differentiation. The planarian *Schmidtea mediterranea* is an excellent model for the *in vivo* study of the molecular mechanisms underlying stem cell differentiation during regeneration. However, how this process is regulated genetically and epigenetically is not well-understood yet. We identified 5 distinct *Smed-cbp* genes in *S. mediterranea* that show different expression patterns. Functional analyses revealed that *Smed-cbp-2* appears to be essential for stem cell maintenance. On the other hand, the silencing of *Smed-cbp-3* resulted in the growth of blastemas that were apparently normal, but remained largely unpigmented and undifferentiated. *Smed-cbp-3* silencing also affected the differentiation of several cell lineages including neural, epidermal, digestive, and excretory cell types. Finally, we analysed the predicted interactomes of CBP-2 and CBP-3 as an initial step to better understand their functions in planarian stem cell biology. Our results indicate that planarian *cbp* genes play key roles in stem cell maintenance and differentiation.

1. Introduction

How stem cells are maintained and differentiate into their multiple distinct lineages remains an open question. Animals that are capable of regenerating offer us the opportunity to study stem cell behaviour *in vivo* in a context in which they are used to rebuild tissues, organs, or large and complex body parts. Among the models capable of whole-body regeneration, freshwater planarians are particularly attractive in that they rely on a population of pluripotent adult stem cells, called neoblasts (Baguñà, 2012; Rink, 2013; Reddien, 2018). In response to any type of incision or amputation in planarians, the wound is closed by muscle contraction in just a few minutes (Chandebois, 1980; Baguñá et al., 1988). Subsequently, a rapid wound response followed by a later regenerative response trigger a programme that activates neoblast proliferation and differentiation, together with cell death and the re-establishment of proper polarity (Saló and Baguñà, 1984; Iglesias et al., 2008; Molina et al., 2007, 2011; Gavino et al., 2011; Pellettieri et al., 2010; Wenemoser and Reddien, 2010; Sandmann et al., 2011; Wenemoser et al., 2012; Owlarn et al., 2017). In recent years, several studies have proven that neoblasts constitute a highly complex and heterogeneous cell population (Scimone et al., 2014; Zhu and Pearson, 2016). A small percentage of neoblasts, the so-called cNeoblasts (clonogenic neoblasts), are true pluripotent stem cells: when transplanted individually into planarians that have been irradiated (and therefore completely depleted of

* Corresponding author. Department of Genetics, Microbiology and Statistics, Faculty of Biology, University of Barcelona, Spain.
E-mail address: fcebrias@ub.edu (F. Cebrià).
[1] equally contributed.

https://doi.org/10.1016/j.ydbio.2021.02.008
Received 5 November 2020; Received in revised form 23 February 2021; Accepted 24 February 2021
Available online 24 March 2021

neoblasts), they are capable of repopulating the host and differentiating into any and all of the planarian cell types (Wagner et al., 2011). A recent study that further characterised these cNeoblasts showed that they express a tetraspanin gene, which constitutes the first specific molecular marker of pluripotent neoblasts (Zeng et al., 2018). However, little is known about how neoblasts are directed to differentiate into their multiple potential lineages (Zhu et al., 2015; Barberán et al., 2016). Post-translational modifications, chromatin remodelling, and epigenetic regulation have important functions in stem cell biology (Avgustinova and Benitah, 2016; Godini et al., 2018; Wang et al., 2014). Interestingly, some planarian studies have uncovered roles of histone and non-histone post-translational modifications in neoblast biology (Dattani et al., 2019; Strand et al., 2019). In *Schmidtea mediterranea,* silencing of different components of the nucleosome remodelling and deacetylase (NuRD) complex such as *Smed-CHD4* (Scimone et al., 2010), *Smed-HDCA-1* (Robb and Sánchez Alvarado 2014), *Smed-RbAP48* (Bonuccelli et al., 2010), and *Smed-p66* (Vásquez-Doorman and Petersen 2016) results in defects in neoblast proliferation and differentiation. Inhibition of ubiquitination and SUMOylation impairs normal neoblast biology and regeneration (Henderson et al., 2015; Strand et al., 2019; Thiruvalluvan et al., 2018). Also, it has been reported that the planarian homologues of the COMPASS family of MLL3/4 histone methyltransferases participate in neoblast proliferation and differentiation and play a conserved role as tumour suppressor genes in these animals (Mihaylova et al., 2018). Finally, some authors have proposed the conserved presence of bivalent promoters in planarian neoblasts (Dattani et al., 2018).

The conserved CBP/p300 family is composed of 2 related transcriptional co-activating proteins: CREB-binding protein (CBP) and p300 (Lundblad et al., 1995), which interact with numerous transcription factors to regulate the expression of their target genes. CBP/p300 proteins achieve their function by acetylating histones and non-histone proteins and by serving as scaffold proteins to bring together different factors within the promoter regions. They are members of the lysine acetyltransferase type 3 (KAT3) family (Dutto et al., 2018), which is present in many organisms including mammals, worms, flies, and plants (Yuan and Giordano, 2002). This family interacts with many cell signalling pathways, such as Notch (Brai et al., 2015), NFkB (Wen et al., 2010), calcium (Hardingham et al., 2001), and TrkB (Esvald et al., 2020) pathways, carrying out its function by interacting with multiple transcription factors and other regulatory proteins (Bedford et al., 2010). The CBP/p300 protein family has been shown to participate in many cellular processes, including cell self-renewal, proliferation, survival, differentiation, synaptic plasticity, the DNA damage response, and cell cycle regulation (Shaywitz and Greenberg, 1999; Giordano and Avantaggiati, 1999; Mayr and Montminy, 2001; Goodman and Smolik, 2000; Manegold, P. et al., 2018; Chan and La Thangue, 2001). In this paper, we describe the identification and characterisation of 5 *cbp* homologue genes in *S. mediterranea*. Whereas *Smed-cbp-2* appears to be required for stem cell maintenance, *Smed-cbp-3* is necessary for the differentiation of several cell lineages, including the central nervous system (CNS), epidermal, gut, and protonephridia. Based on known interactions between CBP/p300 proteins and numerous factors in humans, we used the web application PlanNET (Castillo-Lara and Abril, 2018) to predict the interactome of planarian CBP proteins and identified several interactions that could shed light on the role of these genes during planarian regeneration.

2. Results

2.1. CBP/p300 family in Schmidtea mediterranea

By searching the currently available genome (Grohme et al., 2018), we identified 5 *cbp* homologues in *S. mediterranea*, which we named *Smed-cbp-1, -2, -3, -4* and *-5*. Phylogenetic analysis showed that planarian CBP homologues grouped together, suggesting that they originated from duplications of the *cbp* gene within the Platyhelminthes lineage (Fig. S1).

To characterise their expression patterns, whole mount *in situ* hybridisation (WISH) was performed in intact and regenerating animals (Figs. 1 and S2). In intact planarians, *cbp-1,* and *-4* were expressed rather ubiquitously, mainly in the mesenchyme and the central nervous system (CNS) whereas *cbp-5* was expressed in the mesenchyme around the pharynx (Fig. S2). On the other hand, *Smed-cbp-2* and *-3* showed a broad expression in intact animals including the parenchyma and the CNS (Fig. 1). The expression of both genes decreases after irradiation suggesting that they were expressed in neoblasts (Fig. 1A). During regeneration *cbp-2* and *cbp-3* were expressed in the newly formed brain primordia from early stages (Fig. 1A). Two recent studies have used single-cell sequencing to generate planarian cell-type atlases (Plass et al., 2018; Fincher et al., 2018). These resources allow *in silico* analysis of the expression dynamics of planarian genes over pseudotime in cell types pertaining to specific cell lineages. Single-cell analyses of the expression of planarian *cbp* genes largely agreed with the patterns obtained after WISH (Figs. 1B and S2). Also, analysis of single cell data from distinct neoblast populations indicate that *Smed-cbp-2* and *Smed-cbp-3* were expressed in several neoblast subclasses in agreement with their attenuated expression after irradiation (Fig. 1C). For muscle, neuronal, pharynx, and protonephridia lineages *cbp-1*, *cbp-2,* and *cbp-3* displayed similar dynamics and showed increasing levels of expression during the differentiation process. Conversely, the high levels of expression of *cbp-4* and *cbp-5* in early stages appeared to decay in parallel with the differentiation of progenitor cell types towards distinct cell lineages (Fig. S3).

CBP and p300 have similar structures and share a modular organisation with 5 protein interaction domains (Fig. 1D; Wang et al., 2013). In the middle of the sequence there is a chromatin association and modification region, which encompasses the lysine acetyltransferase domain HAT-K11 and the bromodomain. Thanks to their lysine acetyltransferase activity, CBP and p300 can acetylate both histones and non-histone factors (Dancy and Cole, 2015). The central region is flanked by a characteristic structure composed of several transactivation domains: a transcriptional-adaptor zinc-finger domain 1 (TAZ1); a kinase inducible domain of CREB interacting domain (KIX); a domain of unknown function (DUF); a zz-type zinc finger domain (ZZ); a transcriptional-adaptor zinc finger domain 2 (zf-TAZ); and a IRF3-binding domain (IBiD). *S. mediterranea* CBP proteins contain most of these essential conserved domains (Fig. 1D).

2.2. cbp-2 and cbp-3 are required for proper regeneration

To characterise the function of *Smed-cbp* genes we performed RNA interference (RNAi)-based functional analyses. No obvious defects were observed after silencing *cbp-1*, *-4,* or *-5* (Fig. S4). Conversely, silencing of *cbp-2* or *cbp-3* significantly impaired the viability or regeneration of the treated animals.

Animals treated with *cbp-2* RNAi failed to form a proper blastema (Fig. 2A) and all died within less than 15 days of amputation. On day 5 of regeneration, control animals had already differentiated eyes, whereas *cbp-2*(*RNAi)* animals showed no signs of eye differentiation. After 10 and 12 days of regeneration, *cbp-2(RNAi)* animals differentiated smaller and aberrant eye-pigment cups within very small blastemas that were located closer to the pre-existing post blastema region whereas some of them started to die (Fig. 2A). The efficiency of RNAi silencing was evaluated by qPCR after 7 days of regeneration (Fig. S5).

As *cbp-2(RNAi)* animals failed to regenerate and died, and in order to investigate whether cell proliferation was affected, we carried out immunostaining with anti-phospho-histone-3 (PH3) antibody (that labels proliferating cells at the G2/M transition) in control and *cbp-2(RNAi)* animals. *S. mediterranea* presents 2 mitotic peaks during the regenerative response: the first mitotic peak is global and occurs 6 h after amputation; the second mitotic peak occurs 48 h after amputation and is restricted to a narrow region of the post-blastema adjacent to the wound region (Saló and Baguñà, 1984; Wenemoser and Reddien, 2010). We quantified the number of mitoses at several time points after head amputation (Fig. 2B).

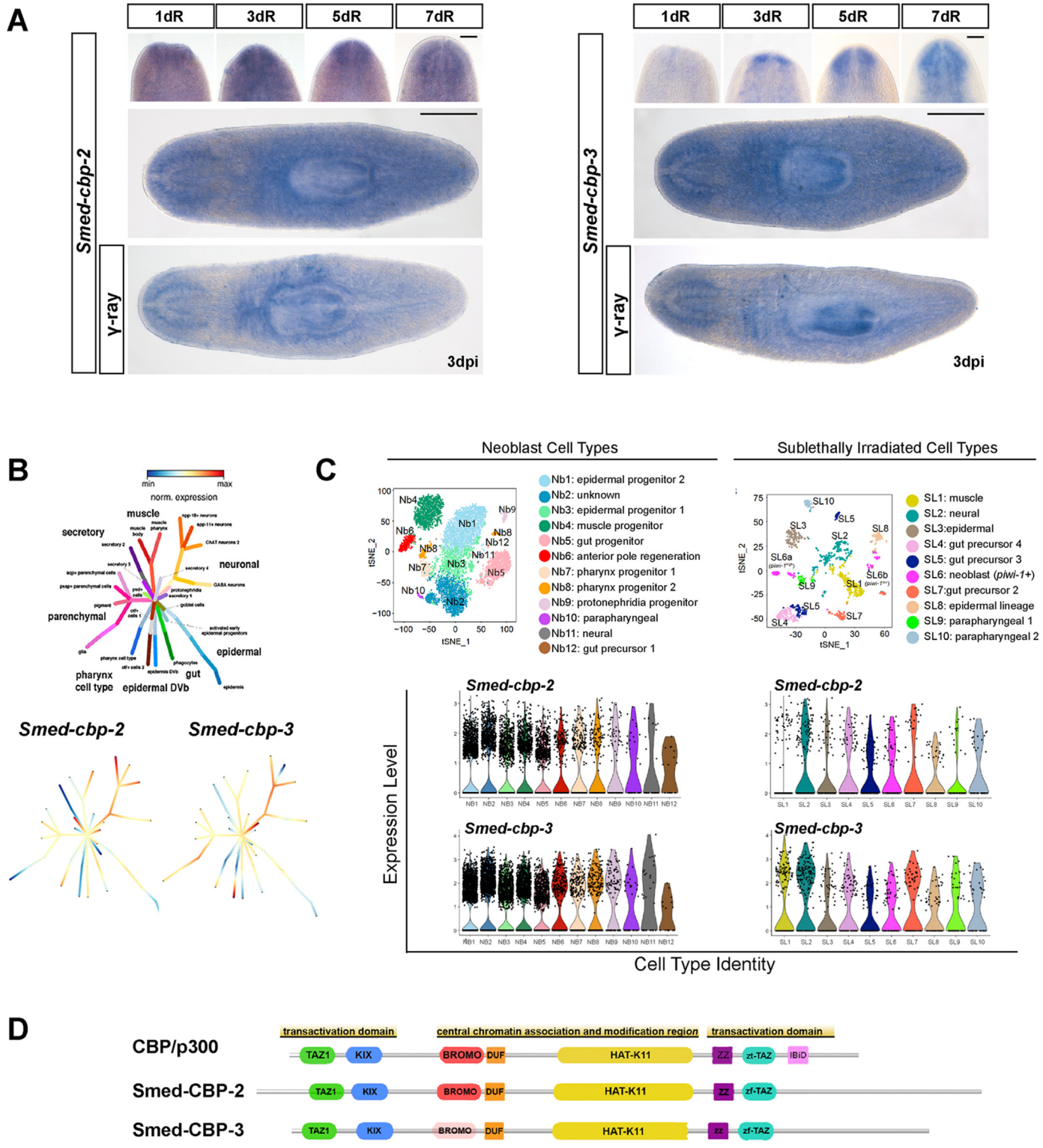

Fig. 1. *Schmidtea mediterranea cbp-2* and *cbp-3* genes. (A) Expression patterns of *Smed-cbp-2* and *Smed-cbp-3* genes as determined by whole mount *in situ* hybridisation (WISH) in intact, regenerating and γ-ray treated planarians. Scale bar: 200 μm in regenerating animals and 400 μm in intact planarians. The anterior end of the body is oriented upwards in regenerating animals and to the left in intact animals. (B) Schematic representation of single-cell transcriptomic expression of *Smed-cbp-2* and *-3* in all planarian cell types (according to Plass et al., 2018). (C) Schematic representation of single-cell transcriptomic expression of *Smed-cbp-2* and *-3* in all planarian neoblasts (Nb) and sublethally irradiated (SL) cell types (according to Zeng et al., 2018). (D) Schematic comparing the domain arrangement of the *S. mediterranea* CBP-2 and CBP-3 proteins with vertebrate CBP/p300. The distinct domains are highlighted in different colours. Faded highlighting of the bromodomain of Smed-CBP-3 denotes weak conservation.

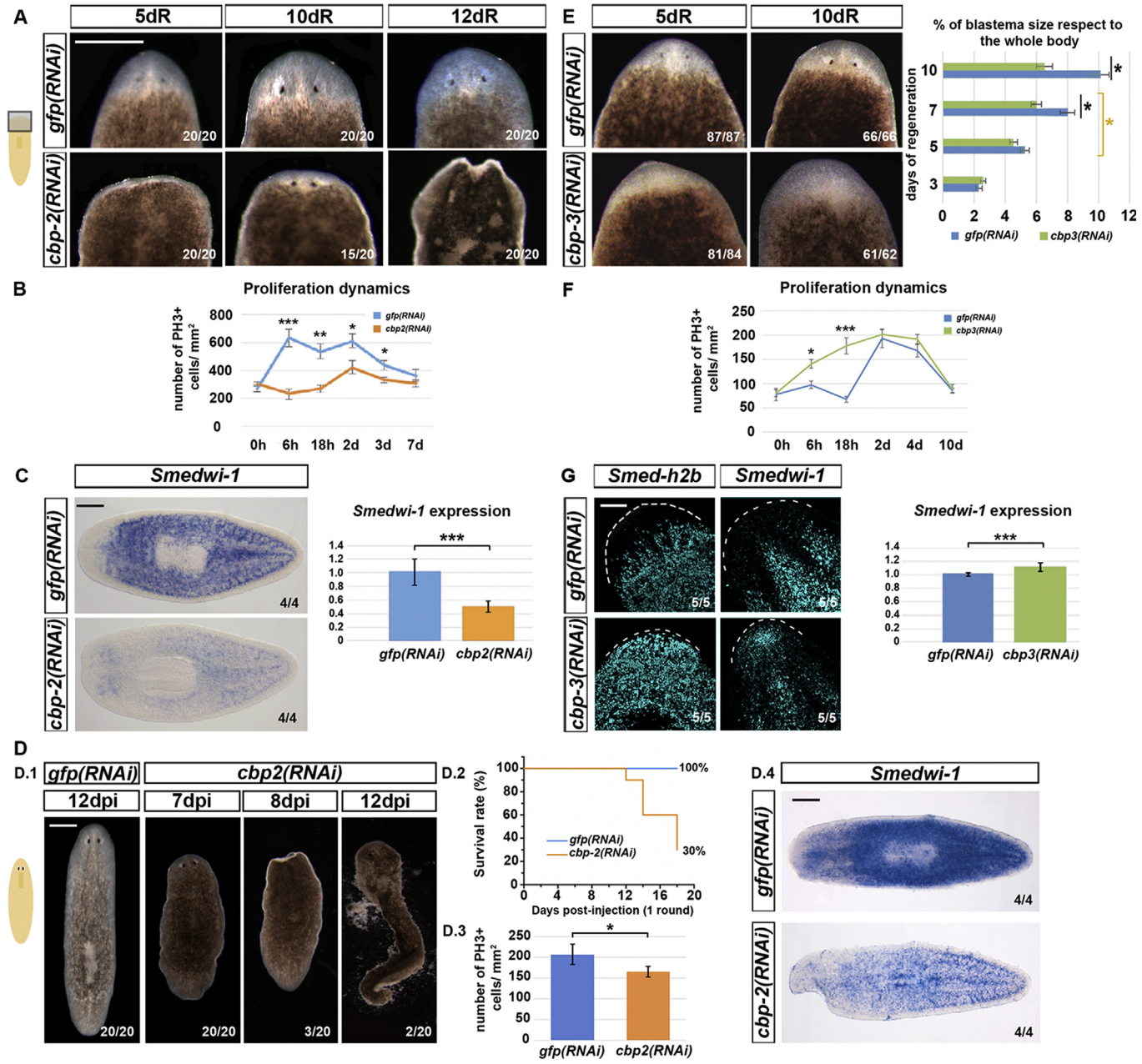

Fig. 2. Defects in regeneration and neoblast pool and proliferation after *cbp-2* and *cbp-3* silencing. (A, E) Live *cbp-2(RNAi)* (A), *cbp-3(RNAi)* (E) and *gfp(RNAi)* animals. Regenerating trunk pieces from *cbp-2(RNAi)* animals fail to form a proper blastema but do differentiate eyes. At 10–12 days of regeneration (dR), they start to die, making wounds all along the body. On the other hand, *cbp-3(RNAi)* animals grow unpigmented blastemas with no signs of eye differentiation. Quantification of blastema size measured as the percentage of the blastema area compared to the total body area. Black asterisks: comparison of *cbp-3(RNAi)* versus control animals at the same time point. Orange asterisk: comparison of *cbp-3(RNAi)* animals at 5 and 7 days of regeneration (values represent the mean ± s.e.m of 30 samples per time point; *p-value<0.05, Student's t-test). Scale bar: 400 μm. (B, F) Quantification of mitotic PH3^{+} immunolabeled cells after silencing *cbp-2* (B) and *cbp-3* (F) at several time points post-amputation. h, hours; d, days (*p-value <0.05; ** p-value<0.01 ***p-value<0.001. Student's t-test. Values represent the mean ± standard error of the mean [s.e.m] of a mean of at least 7 samples per time point and condition). (C) *cbp-2* silencing results in a marked decrease in the neoblast population labelled with *Smedwi-1* at 7 dR. Scale bar: 300 μm. Also, *Smedwi-1* expression, as quantified by qPCR, is significantly decreased after *cbp-2(RNAi)* at 7 dR (***p-value <0.0005). (D) Effects of *cbp-2* silencing during homeostasis. (D.1) Live animals. (D.2) Survival rate after *cbp-2* silencing (n = 20 animals). (D.3) Quantification of mitotic PH3^{+} immunolabeled cells after silencing *gfp*(RNAi) and *cbp-2*(RNAi) at 8 days post-injection. At least 7 animals of each group were analysed. P-value < 0.05. (D.4) *Smedwi-1* WISH at 10 dR after *cbp-2* silencing denotes a marked decrease in the neoblast population. Scale bars: 300 μm. (G) Neoblasts labelled with *Smed-h2b* and *Smedwi-1* accumulate within the blastema of *cbp-3(RNAi)* animals at 10 dR. Dashed lines delimit the tip of the head. Scale bar: 100 μm qPCR analyses reveal increased expression of the neoblast marker *Smedwi-1* after *cbp-3* RNAi at 7 dR. (***P < 0.0005).

Although mitotic neoblasts were detected after *cbp-2* RNAi (Fig. S5), a significant reduction in proliferating cells was observed at all time points. After silencing *cbp-2* the first mitotic peak was not detected, while the second peak at 48 h was significantly attenuated compared to controls. WISH with the neoblast marker *Smedwi-1* revealed a marked decrease in the neoblast population 7 days post-amputation compared with controls, suggesting an important role of *cbp-2* in maintenance of the stem cell population (Fig. 2C). qPCR also revealed a decrease in *Smedwi-1* expression (Fig. 2C). Silencing of *cbp-2* in intact non-regenerating animals also resulted in a reduction in cell proliferation together with death within 2–3 weeks (Figs. 2D and S5). Overall, these results indicate that *cbp-2* is required for survival and suggest an important role of this gene in neoblast maintenance.

On the other hand, RNAi silencing of *cbp-3* resulted in blastemas that grew in size but did not show any external signs of differentiation in terms of eyes or body pigmentation (Fig. 2E). Up to 5 days post-amputation, the blastema of *cbp-3(RNAi)* animals grew at the same rate as that of controls. Subsequently, the blastemas continued to grow but at a slower rate compared to controls (Fig. 2E). The efficiency of *cbp-3* RNAi was quantified by qPCR (Fig. S5). Next, we examined the mitotic response of neoblasts to amputation (Figs. 2F and S5). Remarkably, the first mitotic peak that occurs at 6h as a normal wound response was significantly increased after *cbp-3* silencing (Fig. 2F). Moreover, in *cbp-3*(RNAi) animals proliferation continued to increase from the moment of amputation up until 48 h. This was in marked contrast to controls, in which the first mitotic peak is normally followed by a decrease in proliferative activity up until 18 h, after which proliferation increases again to reach a second mitotic peak at 48 h. After 48 h, the proliferation rate decreased at the same rate as in controls and no further differences were detected (Fig. 2F). Previous studies have demonstrated that the blastema is formed by the entry of neoblasts, which subsequently leave the cell cycle and differentiate to form the multiple missing cell types (Reddien, 2013; Scimone et al., 2014). Given that *cbp-3(RNAi)* animals showed blastemas with no signs of external differentiation and apparently unimpaired neoblast proliferation, the cellular composition of those blastemas was analysed using different neoblast specific markers (Fig. 2G). After 10 days of regeneration, control animals showed a normal distribution of neoblasts, which were largely absent from the blastema. By contrast, the blastemas of *cbp-3(RNAi)* animals contained abundant neoblasts (Fig. 2G), suggesting that *cbp-3* silencing impairs neoblast differentiation within the blastema. qPCR analyses also showed an increase in the expression levels of the neoblast markers *Smedwi-1* and *soxp-2* after *cbp-3* RNAi (Figs. 2G and S5). In intact animals *cbp-3* silencing did not result in any obvious phenotype in terms of external morphology, gut or CNS morphology, and had no effect on the rate of neoblast proliferation (Fig. S6).

Finally, the expression of polarity determinants such as *Smed-wntp1* and *Smed-notum* was also analysed (Reddien, 2018). No major defects were observed for these markers at 12h of regeneration where polarity is established (Fig. S7). After 7 days of regeneration decreased expression was observed for *Smed-wntp1* after *cbp-3* RNAi. Also, the expression of *Smed-notum* in the anterior pole, mainly the expression associated with the CNS was reduced in these animals (Fig. S7).

2.3. Defective CNS regeneration after cbp-2 and cbp-3 RNAi

We next used specific markers to analyze the differentiation of several cell types and tissues within the blastemas of the *cbp-2* and *cbp-3* RNAi

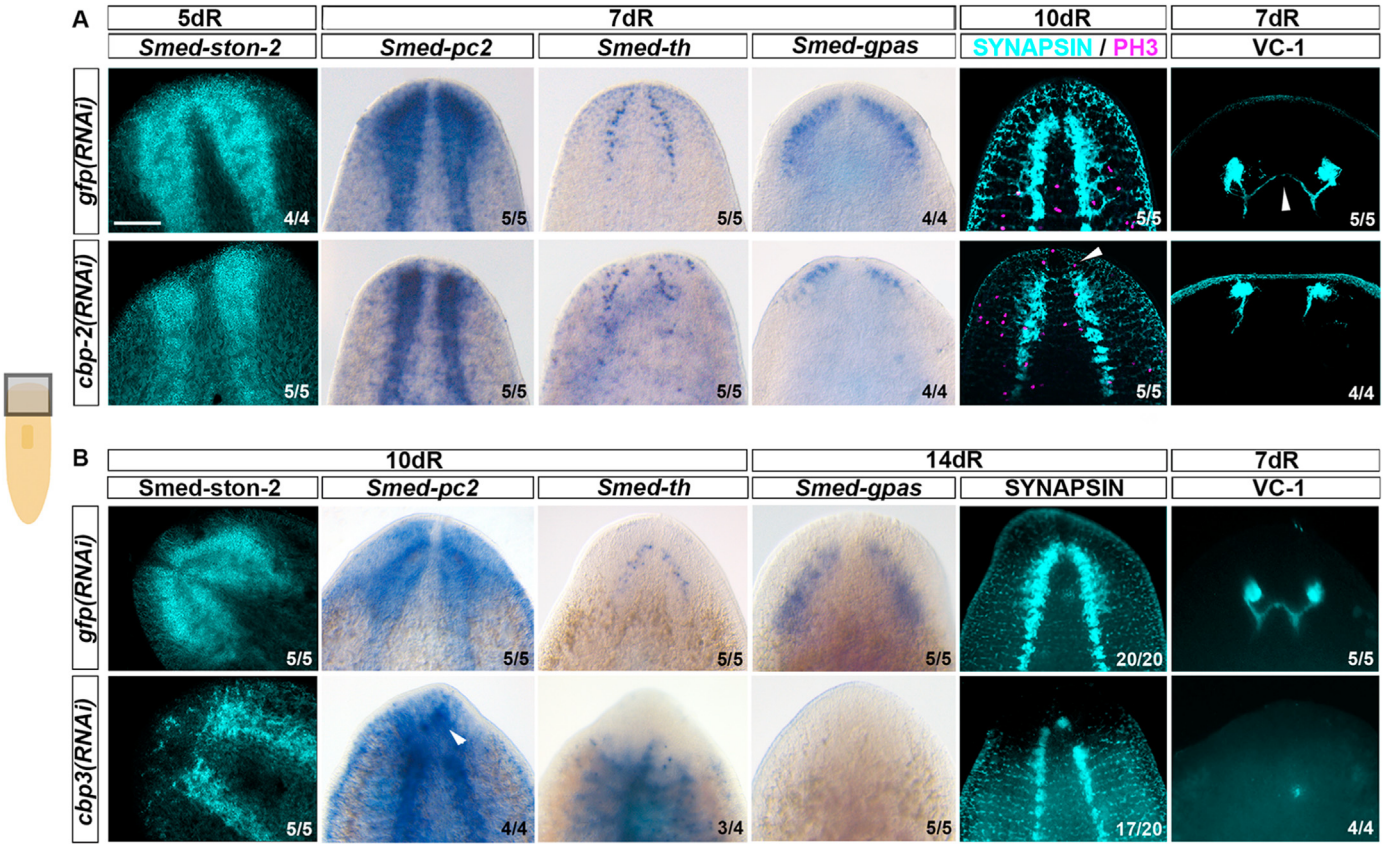

Fig. 3. Neural differentiation defects after *cbp-2* and *cbp-3* silencing. (A) CNS regeneration, visualised by *Smed-ston-2, Smed-pc2, Smed-th, Smed-gpas* WISH and anti-SYNAPSIN immunostaining, is strongly disrupted in regenerating trunks from *cbp-2*(RNAi) animals after 5–10 dR (days of regeneration). Moreover, these treated animals show an abnormal anterior distribution of mitoses (white arrowhead). The visual system, as visualised by VC-1 immunostaining, shows an abnormal pattern with no optic chiasm (arrowhead). (B) *cbp-3* silencing inhibits CNS differentiation as visualised with the same neural specific markers, evaluated between 10 and 31 dR. VC-1 immunostaining reveals a total absence of the photoreceptors differentiation. Scale bar: 300 μm.

animals. First, we analysed in detail the differentiation of the CNS and photoreceptors after *cbp-2* and *cbp-3* silencing. Although *cbp-2(RNAi)* animals were able to differentiate new photoreceptor cells (Fig. 2), unlike controls, visual axons failed to extend to form a proper optic chiasm (arrowhead in Fig. 3A). Interestingly, in *cbp-2(RNAi)* animals differentiation of brain tissue occurred in the wound region (Fig. 3A). However, in line with our observations in photoreceptors, the new brain cells did not form properly patterned cephalic ganglia; the 2 small brain rudiments were not connected by a transverse commissure and were located mainly in the pre-existing post-blastema region. Also, a reduction for dopaminergic (*Smed-th*) and brain lateral branches (*Smed-gpas*) neurons was observed (Fig. 3A) Moreover, whereas in controls mitotic cells were normally observed behind the new cephalic ganglia, in *cbp-2(RNAi)* animals proliferating neoblasts were detected at the tip of the head, in front of the newly differentiated brain tissues (arrowhead in Fig. 3A).

In *cbp-3(RNAi)* animals, labelling with pan-neural markers such as *Smed-pc2* and SYNAPSIN revealed markedly impaired regeneration of new cephalic ganglia (Fig. 3B). In agreement with these observations dopaminergic (*Smed-th*), and brain lateral branch (*Smed-gpas*) neurons were completely absent or significantly reduced in *cbp-3*(RNAi) animals (Fig. 3B). Moreover, when cells positive for these markers were detected within the blastema their pattern was altered compared with that of controls (Fig. 3B). Finally, in accordance with the lack of eye-pigment cells no photoreceptors were observed after immunostaining with VC-1 (Fig. 3B). Defects in the posterior regeneration of the CNS were also observed after *cbp-2* and *cbp-3* RNAi (Fig. S8).

2.4. Non-neural defects after cbp-2 and cbp-3 RNAi

Next, we used different specific markers to analyze the differentiation of non-neural tissues after the silencing of *cbp-2* and *cbp-3* (Figs. 4 and S8). While regenerating head pieces showed normal extension of new posterior gut branches and formed a pharynx cavity (Fig. S8), most *cbp-2(RNAi)* animals failed to regenerate proper ventral nerve cords and pharynges (Fig. S8). During anterior regeneration, differentiation of the digestive and excretory system within the blastema was unaffected (Fig. 4A). Similarly, the expression of the marginal mature epidermal cells marker *Smed-ifb* and the muscle marker TMUS13 did not reveal differences compared to controls (Fig. 4A). Planarian epidermal cells are multi-ciliated cells (Hyman, 1951) and exhibit distinct patterns on dorsal and ventral surfaces. Dorsally, ciliated epidermal cells are mainly distributed along the midline and the lateral sides of control animals; ventrally, these ciliated epidermal cells show a uniform distribution (Fig. 4B). In *cbp-2* RNAi animals, anti-tubulin immunostaining revealed more disorganised cilia along the midline of the dorsal epidermis as compared with controls (Fig. 4A). On the other hand, *cbp-3(RNAi)* animals failed to differentiate new excretory (*Smed-innexin-10*), marginal epidermal cells (*Smed-ifb*) (Fig. 4B) and pharynges (Fig. S8). The morphology of the regenerated primary gut branches (*Smed-pk*) was aberrant compared to controls, with no obvious secondary ramifications (Figs. 4B and S8). However, silencing of *cbp-3* appeared not to impair normal regeneration of the body-wall musculature: cells in the corresponding blastemas differentiated to form circular, longitudinal, and

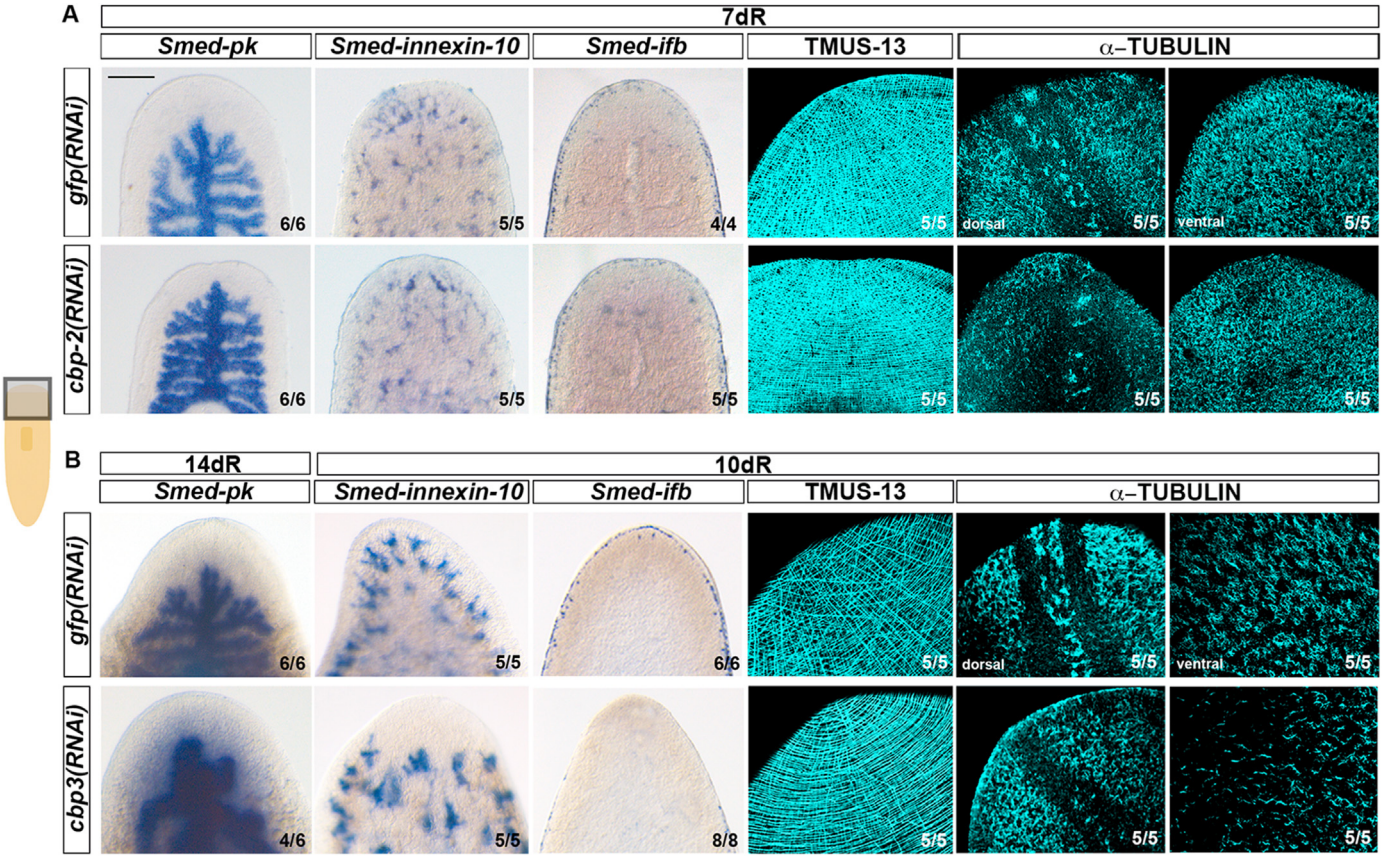

Fig. 4. Non-neural defects after *cbp-2* and *cbp-3* silencing. (A) Digestive and excretory system regeneration, visualised by WISH for *Smed-pk* and *Smed-innexin-10,* respectively, is not affected after *cbp-2* silencing in regenerating trunks after 7 dR (days of regeneration). No differences in the expression of *ifb* in the epidermal cells along the dorsoventral margin or the body wall musculature (TMUS-13) are observed between control and *cbp-2(RNAi)* animals. Anti-TUBULIN immunostaining reveals an abnormal pattern of cilia along the dorsal midline in *cbp-2(RNAi)* animals. (B) The anterior gut branch fails to properly differentiate after *cbp-3* silencing and protonephridial and epidermal *ifb* + cells are absent in *cbp-3(RNAi)* animals after 10 dR. Normal regeneration of the body wall musculature after cbp-3 RNAi. Anti-TUBULIN immunostaining reveals fewer, disorganised cilia in *cbp-3*(RNAi) animals after 10 dR. Scale bar: 200 μm in all images, except, 100 μm for TMUS-13 and TUBULIN. In all images, the anterior end is oriented upwards.

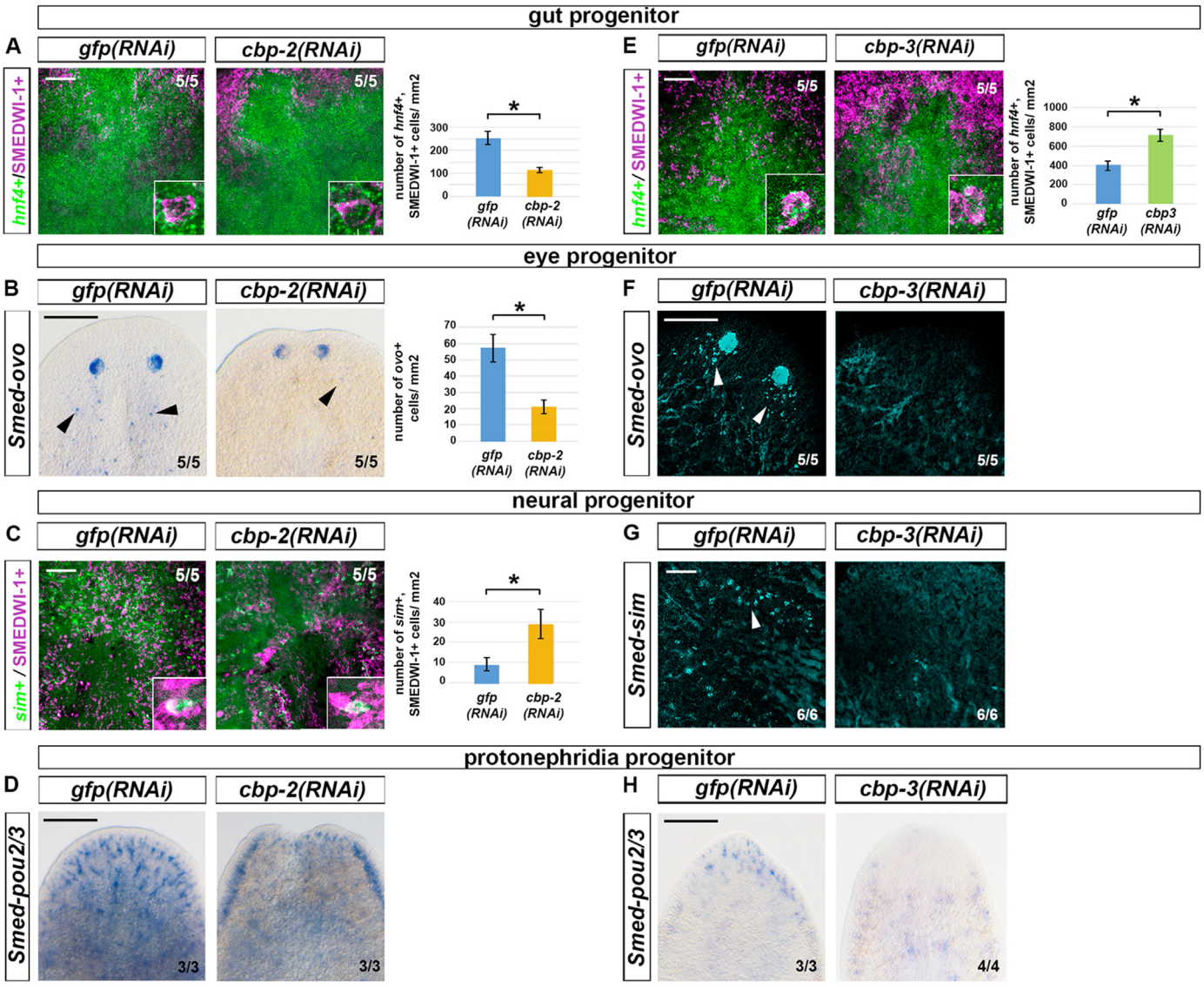

Fig. 5. Defects in cell progenitor compartments after *cbp-2* and *cbp-3* silencing. (A, E) Double FISH and immunostaining and quantification of *Smed-hnf4*/SMEDWI-1+ gut progenitors. The inset in each panel shows a magnified view of the progenitor cells. Gut progenitors significantly decrease in *cbp-2*(RNAi) animals (A) and increase in *cbp-3*(RNAi) animals (E). (B, F) Knockdown of *cbp-2* causes a significant decrease in the number of eye progenitors cells (arrowheads) labelled with *Smed-ovo* (B). On the other hand, eye progenitors are undetectable in *cbp-3*(RNAi) animals (F). (C, G) *cbp-2* silencing (C) results in a significant increase in neural progenitors double labelled with *Smed-sim/SMEDWI-1 and are* undetectable after *cbp-3* silencing (G). (D, H) *Smed-POU2/3*/SMEDWI-1 double labelled protonephridial progenitors decrease within the blastemas of *cbp-2*(RNAi) animals (D) and are absent in *cbp-3*(RNAi) animals (H). In all cases, *P < 0.05 (Student's t-test). Values represent the mean ± s.e.m of at least 5 samples per condition. Scale bars: 100 μm in A, C, E and G, 200 μm in B, D, F and H. All images correspond to samples at 10 days of regeneration.

diagonal muscle fibres (Fig. 4B). Even though epidermal cells differentiated within the blastemas of *cbp-3(RNAi)* animals they appeared to regenerate epidermal cells with a reduced number of cilia and lacked the typical dorsal stripe (Fig. 4B). Overall, these results indicate that *cbp-3* RNAi significantly alters the differentiation of neural, gut, and excretory cells. However, in *cbp-3(RNAi)* animals the body-wall musculature regenerated normally and new epidermal cells appeared within the blastema, albeit with defective cilia.

2.5. *cbp-2 and cbp-3 RNAi affects specific progenitor populations*

To characterise the impact of the decrease in the neoblast population after the silencing of *cbp-2* on the specification of distinct populations of progenitors, we performed double-labelling for cell progenitor-specific markers and the neoblast marker anti-SMEDWI-1 (Fig. 5). Using *Smed-hnf-4* (Wagner et al., 2011) and *Smed-ovo* (Lapan and Reddien, 2012) as specific markers for gut and eye progenitors, respectively, we observed a significant reduction in the numbers of these progenitors after *cbp-2* silencing (Fig. 5A and B). The number of *sim* + neural progenitors (Cowles et al., 2013) increased significantly after silencing *cbp-2* (Fig. 5C). Finally, the expression of the protonephridial progenitor marker *Smed-pou2/3* (Scimone et al., 2011) was also decreased after silencing *cbp-2* (Fig. 5D). In agreement with the observed reduction in the neoblast pool, these results suggest that different populations of cell specific progenitors decrease after *cbp-2* silencing. Taken together with the findings described in the previous section, these data suggest that while *cbp-2* RNAi results in either a decreased (gut and eye) or increased (neural) number of certain progenitors, the new mature cells that

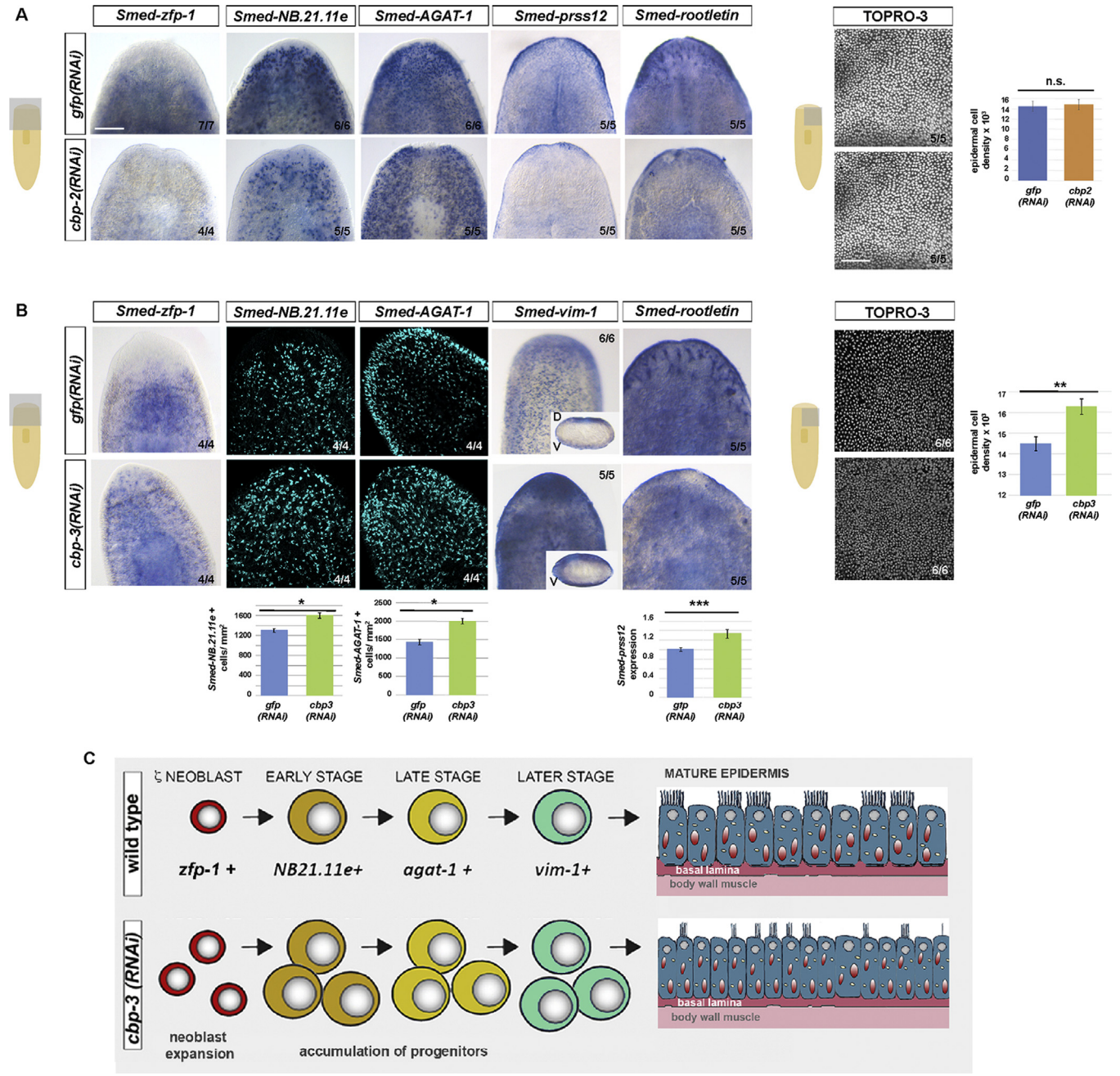

Fig. 6. Defects in the epidermal lineage after *cbp-2* and *cbp-3* silencing. (A) *cbp-2* RNAi causes an evident decrease in ζneoblasts (*zfp-1+)* and early- and late-stage epidermal progenitors (*Smed-NB.21.11e* and *Smed-AGAT-1*, respectively). Reduced *Smed-rootletin* and *Smed-PRSS12* expression in the differentiated epidermal cells is also observed after *cbp-2* silencing. Epidermal cell density as visualised with TO-PRO®-3 is not affected after *cbp-2* silencing. **(B)** The number of epidermal progenitors, labelled for *Smed-zfp-1, NB.21.11.e,* and *AGAT-1*, increase significantly after *cbp-3* knockdown p-value < 0.05. *Smed-vim-1+* cells and *Smed-PRSS12* expression quantified by qPCR significantly increase after *cbp-3* silencing (p-value < 0.0005). Smed-rootletin expression decreases after *cbp-3* knockdown. Epidermal nuclear density increases after *cbp-3* silencing, as visualised with TO-PRO®-3 (p-value < 0.01). **(A–B)** Scale bar: 200 μm for WISH images and 100 μm for WFISH and TO-PRO®-3 images. All samples correspond to regenerating trunks after 7 (for *cbp-2*) and 10 (for *cbp-3*) days of regeneration. In all images, the anterior end is oriented upwards. **(C)** Schematic summarising the main defects along the epidermal lineage after *cbp-3* silencing.

differentiate from these progenitors fail to give rise to properly patterned tissues and organs.

In the case of *cbp-3* its silencing did not result in a reduction of the neoblasts but, on the contrary, an increase of them within the blastemas (Fig. 2G). To determine whether the defects observed in cell differentiation were the result of a lack of or a reduction in the number of lineage-committed progenitors, or were due to defective differentiation into mature cells, we analysed the expression of different progenitor-specific markers (Fig. 5). The *cbp-3* silencing resulted in an increase in gut progenitor cells (Fig. 5E). However, proper gut regeneration was not observed (Figs. 4B and S8), suggesting that *cbp-3* may be required for the differentiation, but not the specification, of the gut progenitor cells. On the other hand, whereas controls displayed *Smed-ovo* + mature photoreceptors and eye progenitors, this marker was absent in *cbp-3(RNAi)* animals (Fig. 5F); moreover, analyses of the expression of neural and excretory progenitor markers revealed a complete absence of both within the blastema after *cbp-3* silencing (Fig. 5G and H). Finally, *Smed-sim* + neurons were practically absent in the mesenchyme of intact planarians after *cbp-3*

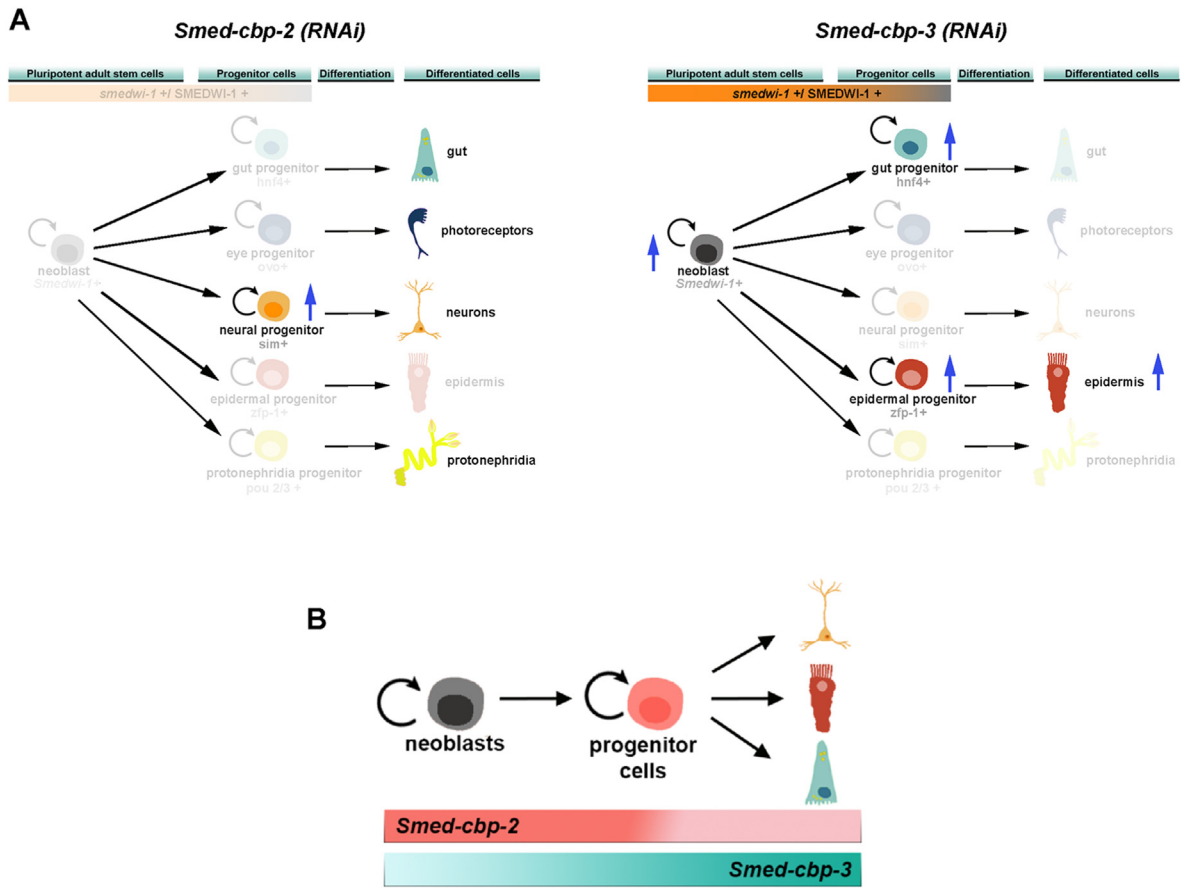

Fig. 7. Schematic representation of the defects observed in the different cell compartments and lineages after silencing *cbp-2* and *cbp-3*. (A) Compared to controls, after the silencing of *cbp-2* the number of neoblasts as well as gut, eye, epidermal and protonephridial progenitors decrease. Neural progenitors, however, increase. After the silencing of *cbp-3* the number of neoblasts and gut and epidermal progenitors increase. Eye, neural and protonephridia progenitors decrease and epidermal cell density increases. (B) Proposed model for the functional requirement of *cbp-2* and *cbp-3* along the differentiation pathway.

silencing (Fig. S6). These observations are in line with the marked impairment of CNS regeneration (Fig. 3B) and suggest that *cbp*-3 might be required for neural progenitor specification. Taken together, these results indicate that, during regeneration, *cbp-3* plays different roles in progenitor specification and differentiation depending on the specific cell lineage.

2.6. *cbp-2 and cbp-3 is required for the proper regeneration of the epidermal lineage*

We next performed WISH for several epidermal markers to investigate the role of *cbp-2* during epidermal maturation. Planarian epidermis is a monostratified tissue consisting of a single layer of both non-ciliated and multi-ciliated differentiated cell types (Rompolas et al., 2010). The epidermal lineage is very well characterised in planarians (Zhu et al., 2015; Cheng et al., 2018; Zhu and Pearson, 2018). Epidermal maturation requires temporally correlated transition states in which lineage-committed zeta neoblasts (*Smed-zfp-1*+, van Wolfswinkel et al., 2014) become post-mitotic and begin to sequentially express *Smed-NB.21.11e* (“early progeny progenitor cells”) and *Smed-AGAT-1* (“late progeny progenitor cells’’), and finally differentiate into mature epidermal cells that express genes such as *ifb*, *rootletin*, and *PRSS12* (Wurtzel et al., 2017). RNAi knockdown of *cbp-2* resulted in a reduction in *zfp-1*+ cells (Fig. 6A). In agreement with these findings, we also observed a marked depletion of epidermal progenitor cells after *cbp-2* silencing (Fig. 6A). To evaluate the effects of this decrease in epidermal progenitors on epidermal differentiation, we analysed the expression of specific markers of mature epidermis. In control animals, *Smed-PRSS12* is expressed throughout the dorsal and ventral epidermis in both ciliated and non-ciliated epidermal cells, whereas *Smed-rootletin* is only expressed in ciliated epidermal cells (Wurtzel et al., 2017). After *cbp-2* silencing, expression of both genes was dramatically reduced (Fig. 6A). However, when analyzing cell density within this mono stratified epidermis no significant differences in cell number were observed (Fig. 6A).

In contrast, *cbp-3(RNAi)* animals showed large numbers of *Smed-zfp-1*+ cells within the blastema up to the tip of the head (Fig. 6B) in agreement with our observation that the blastemas of these animals are full of neoblasts. Concomitant with this increase in *Smed-zfp-1*+ neoblasts, we observed a significant increase in the number of *Smed-NB.21.11e*-, *AGAT-1*-, and *vimentin*-positive cells (Fig. 6B). Moreover, while *Smed-PRSS1/2* expression was increased, *Smed-rootletin* expression appeared to be reduced (Fig. 6B) that would agree with the observed decrease in excretory cells and cilia in the epidermis previously shown (Fig. 4B). Remarkably, quantification of epidermal cell density revealed a significant increase in the number of cells in the epidermal monolayer compared with controls (Fig. 6B). However, based on the absence of *ifb* + cells along the dorsoventral border (Fig. 4B) and the defects observed in the cilia (Fig. 4B), these results suggest that *cbp-3* may be required for the final maturation of a subset of epidermal cells (Fig. 6C).

2.7. *Analysis of Smed-cbp-2 and Smed-cbp-3 co-expression and interaction with other factors*

The results described in the previous sections suggest that planarian cbp genes diverged functionally after duplication. *Smed-cbp*-2 might be

Table 1
Summary of *Smed-cbp-2* RNAi and *Smed-cbp-3* RNAi phenotypes. Hpa, hours post-amputation.

			Smed-cbp-2 (RNAi)	Smed-cbp-3 (RNAi)
Blastema Growth		Until 5 days of Regeneration	Almost absent	Normal
		From 5 days of Regeneration	Almost absent	Slower
Animal Survival			Impaired	Not affected
Neoblasts	Proliferation dynamics	1st mitotic peak (6 hpa)	Absent	Increased
		2nd mitotic peak (48 hpa)	Not affected	Not affected
	Smedwi-1 expression		Decreased	Increased
Polarity	Anterior	*notum* (12 hpa)	Not affected	Not affected
	Posterior	*wntp1* (12 hpa)	Not affected	Not affected
Eye cell types	Progenitor cells	*ovo*+	Reduced	Absent
	Mature cells	Pigment cups	Present	Absent
		Photoreceptor cells (VC1+)	Present	Absent
		Optic chiasm (VC1+)	Absent	Absent
Digestive system	Progenitor cells	*hnf4*+/PIWI1+	Decreased	Increased
	Mature cells	*pk*+	Present	Present
		Pharynx regeneration (*laminin*+)	Absent	Absent
	Patterning	Gut ramification	Not affected	Perturbed
Nervous system	Progenitor cells	*sim*+	Increased	Strongly reduced
	Mature cells	Cephalic Ganglia (SYNAPSIN+, *ston-2*+, *pc2*+)	Present	Strongly reduced
		Dopaminergic neurons (*th*+)	Present	Absent
	Brain patterning	Cephalic Branches (SYNAPSIN+, *Gpas*+)	Present	Absent
		Transverse Commissure	Absent	Absent
Excretory system	Progenitor cells	*pou2/3*+	Reduced	Absent
	Mature cells	*innexin-10*+	Present	Absent
Muscular system		TMUS-13	Not affected	Not affected
Epidermal lineage	Progenitor cells	*zfp-1*+	Reduced	Increased
		NB.21.11e+	Reduced	Increased
		AGAT1+	Reduced	Increased
	Mature cells	*prss12*+	Reduced	Increased
		rootletin+	Reduced	Reduced
		ifb + *cells*	Present	Absent
	Epithelial cell density	TOPRO-3	Not affected	Increased
	Cilia	α-TUBULIN	Reduced	Reduced

mainly required for correct neoblast maintenance, whereas *Smed-cbp-3* would regulate commitment of stem cells into specific progenitor lineages as well as their final differentiation into well-patterned differentiated tissues. To gain further insights into these diverse functions, we took advantage of available planarian single-cell data (Plass et al., 2018) and the recently developed Gene Co-expression Counts tool (Castillo-Lara and Abril, 2018; Castillo-Lara et al., 2020) to perform a deeper analysis of the expression of *Smed-cbp-2* and *Smed-cbp-3* in the main planarian cell lineages (Fig. S9).

Our analysis showed that the relative percentage of *Smed-cbp genes*-expressing cells was considerably uniform across lineages, with *Smed-cbp-3* consistently more abundant than *Smed-cbp-2*. Specifically, *Smed-cbp-2* expression in the different lineages ranged from 4.4% in muscle cells to 6.3% in neuronal cells (Fig. S9A). *Smed-cbp3* expression at the single-cell level ranged from 7% in epidermal cells of the dorsoventral boundary to 15% in excretory cells. Both progenitor (*Smedwi-1*+) and differentiated (*Smedwi-1*-) cells of the neuronal, epidermal, muscular, and intestinal compartments expressed *Smed-cbp* genes (Fig. S9B). Interestingly, in most cellular lineages, *Smed-cbp* genes expression was slightly enriched in the progenitor compartment. In particular, in the neural lineage nearly 11% and 13% of neural progenitor cells versus only 5.2% and 9.1% of differentiated neural cells expressed *Smed-cbp-2* and *Smed-cbp-3*, respectively. As mentioned above, planarian cell-type atlases based on single-cell sequencing reveal similar expression dynamics for *Smed-cbp-2* and *Smed-cbp-3* during the differentiation of most planarian cell types (Fig. 1, S3 and S9B). Remarkably, however, we found that only a small percentage of cells (<1% of cells in most cell lineages) co-expressed planarian *Smed-cbp-2* and *Smed-cbp-3* genes, accounting for 9% (175 *cbp-2*$^{+}$*cbp-3*$^{+}$ versus 1941 *cbp-2*$^{+}$cells) and 15% (175 *cbp-2*$^{+}$*cbp-3*$^{+}$ versus 1162 *cbp-2*$^{+}$cells) of the total number of *cbp-2* and *cbp-3* cells analysed, respectively (Fig. S9A). Together, these findings indicate that *Smed-cbp-2* and *Smed-cbp-3* co-expression is minimal.These analyses also revealed that *Smed-cbp-3* was expressed in a higher percentage of cells than *Smed-cbp-2* in all cell lineages and that both genes were expressed in progenitors and fully differentiated cells in all lineages, except for *Smed-cbp-2* in the protonephridia lineage (although we only identified 4 cells expressing this gene) (Fig. S9).

CBP proteins are multifunctional transcriptional co-activators and their diverse functions rely in part on an extended network of protein interactors (Bedford et al., 2010; https://thebiogrid.org; https://string-db.org). To investigate whether the diverse functions of planarian Smed-CBP-2 and Smed-CBP-3 depend on such a network of protein interactors, we used the recently developed PlanNET tool (Castillo-Lara and Abril, 2018), which predicts planarian protein-protein interactions using sequence homology data and a reference Human interactome, to examine the interactome of planarian Smed-CBP-2 and Smed-CBP-3. Surprisingly, in spite of their diversified function, PlanNET predicted similar interactome profiles for planarian Smed-CBP-2 and Smed-CBP-3 (Figs. S10 and S11). The interaction of Smed-CBP-2 and Smed-CBP-3 with several proteins known to be regulated and/or directly acetylated by human CBP/p300 homologues appeared conserved in planarians (Fig. S10). Interestingly, some interactors such as p53, Runx1, and Ets2 have been already functionally characterised in planarians (see references listed in Fig. S10A) and their essential roles in processes such as neoblast proliferation, specification, and differentiation may be related to their regulation by CBPs. Together, these results indicate that despite being expressed in different cells, Smed-CBP-2 and Smed-CBP-3 share a common network of protein interactors, suggesting that their diversified function may depend on the cellular environment in which *Smed-cbp-2* or *Smed-cbp-3* are expressed.

3. Discussion

CREB-binding protein (CBP) and p300 have a central role in regulating gene expression in metazoans. CBP was originally characterised as a binding partner of CREB (cAMP-response element binding) protein (Chrivia et al., 1993). The functions of these proteins are mainly linked to their roles as transcriptional co-activators, serving as scaffolds to bring together different factors at promoter regions, as well as through their lysine acetyltransferase activity. Thus, hundreds of CBP-interacting proteins have been described and dozens of proteins (histone and non-histone) have been shown to be acetylated by CBP/p300 proteins (Dancy and Cole, 2015; Holmqvist and Mannervik, 2013; Voss and Thomas, 2018). Whereas a single homologue of the CBP/p300 family has been identified in cnidarians, flies, molluscs, and non-vertebrate chordates, gene duplication that occurred at the origin of the vertebrate lineage seems to constitute the origin of the CBP and p300 paralogs identified in vertebrates (Thomas and Kahn, 2016). Remarkably, this gene family has been expanded in Platyhelminthes (Fig. S1), similarly as it has been shown for other gene families (Iglesias et al., 2008; Molina et al., 2009; Su et al., 2017).

Although vertebrate CBP and p300 share an extremely high degree of identity, they appear to have non-redundant functions (Thomas and Kahn, 2016). Thus, in the context of mammalian stem cell biology, CBP and p300 have been proposed to regulate proliferation and differentiation through their interaction with β-catenin. A current model based on several findings from a variety of progenitor/stem cells proposes that the interaction of β-catenin with p300 promotes the expression of genes involved in cell differentiation, whereas the interaction of β-catenin with CBP is required for stem cell renewal and maintenance (Thomas and Kahn, 2016; Manegold et al., 2018). Here, we describe 5 *cbp* homologues in *S. mediterranea* that show distinct expression patterns (Figs. 1 and S2). Analyses at the single-cell level along the differentiation pathway of different cell lineages allowed distinction between *Smed-cbp-1*, *-2* and *-3* and *Smed-cbp-4* and *-5*, as the expression of the first group increased, in general, with the transition of neoblasts to fully differentiated cells, whereas the opposite was seen for *Smed-cbp-4* and *-5* (Fig. S3). Interestingly, functional analyses indicate that the silencing of *Smed-cbp-2* and *Smed-cbp-3* yield distinct phenotypes (a comparative summary of the defects observed after their silencing is shown in Table 1). Thus, silencing of *Smed-cbp-2* perturbed regeneration, resulting in a failure to grow normal blastemas. *cbp-2(RNAi)* planarians showed significant reductions in the neoblast population, *Smedwi-1* expression, and the number of proliferating cells (Fig. 2). Despite these defects, neoblasts differentiation appeared to normally occur, which suggests a role of this gene in neoblast maintenance and proliferation. However, a function of *Smed-cbp-2* in directly regulating the expression of neoblast specific genes cannot be completely ruled out. On the other hand, it is also true, that the pattern of the new organs such as the brain and the visual axons is aberrant after silencing *cbp-2*, which suggests additional roles of this gene in patterning. Thus, for example the lack of the optic chiasm could be related to the lack of the transverse commissure between the cephalic ganglia and/or an absent or decrease of notum signal in the guidespot-like cells required for the proper patterning of the visual axons (Scimone et al., 2020).

The silencing of *Smed-cbp-3* mainly resulted in deficient differentiation for several lineages, with blastemas that remained mainly undifferentiated and containing an abnormally high number of neoblasts and increased expression of neoblast markers such as *Smedwi-1* and *Smed-soxp-2* (Fig. 2). Based on these results it is tempting to speculate that *Smed-cbp-2* and *Smed-cbp-3* may have diverged functionally to regulate either stem cell maintenance or differentiation, respectively, as has been described for vertebrate CBP and p300 (Thomas and Kahn, 2016; Manegold et al., 2018). Whether these different functions of planarians *cbp-2* and *cbp-3* could be mediated through the interaction of these factors with the Wnt/β-catenin pathway, as happens in mammalian stem cells, remains to be determined.

Although silencing of *Smed-cbp-2* and *cbp-3* yielded rather different phenotypes the expression patterns of these genes was very similar (Figs. 1 and S3). However, deep *in silico* analyses of an available planarian cell atlas (Plass et al., 2018) clearly indicates that the level of co-expression of these 2 genes is extremely low and quite similar in all cell lineages analysed. Interestingly, for both genes expression in the progenitor compartment (*Smedwi-1* positive) was slightly higher than in the differentiated compartment (*Smedwi-1* negative) (Fig. S9), which would agree with the variety of phenotypes observed after silencing of these genes, in terms of the diversity of cell lineages affected, their probable requirement for progenitor specification, and the final differentiation of several cell types. As discussed above, vertebrate CBP/p300 proteins interact with hundreds of partners. However, the interactomes of CBP and p300 are in general very similar (Bedford et al., 2010; https://thebiogrid.org; https://string-db.org), suggesting that the different functions of these 2 genes are probably not mediated by specific interactions with distinct sets of other proteins, but in fact by the cellular context in which these interactions may occur. Similarly, planarian *cbp-2* and *cbp-3* have very similar predicted interactomes (Fig. S10). Together with the extremely low level of co-expression of these 2 genes, this finding further supports the view that their functions may depend more on the cellular and molecular context than on their specific interacting partners.

It is worth mentioning that the silencing of each of these 2 genes has distinct effects on the different cell lineages analysed. Thus, whereas *cbp-2* silencing resulted in a significant decrease in the *Smedwi-1*+ population of stem cells, which probably explains the subsequent decrease observed in epidermal, gut, and photoreceptor progenitors, we observed an increase in the neural progenitor compartment (Fig. 5). This suggests that *cbp-2* may also play a role in regulating the cell fate of planarian progenitors, similar to its role in *Xenopus* embryos, in which inhibition of CBP/p300 function impairs the differentiation of non-neural tissues while simultaneously inducing neurogenesis throughout the entire embryo (Kato et al., 1999). In planarians, *Smed-soxB1* has been shown to mark ectodermal-lineage progenitors and its activity is required for differentiation of subsets of ciliated epidermal and neuronal cell types (Ross et al., 2018). Interestingly *in silico* analysis of single cell data (Plass et al., 2018) indicate that 11.4% of the *SoxB1*+ cells co-express *cbp-3* and 5,9% co-express *cbp-2*, pointing out the possibility that part of *Smed-SoxB1* function may be regulated by *cbp* genes. Remarkably, we found that silencing of *cbp-2* resulted in the death of all treated animals, both intact and regenerating, suggesting an additional role of *cbp-2* in animal viability. This lethality observed could be a consequence of problems with the integrity of the epidermis as the animals display epidermal wounds before dying (Fig. 2). The normal epidermal cell turnover takes about 7–10 days (Tu et al., 2015). Although we did not observe any difference in epidermal cell density at 7 days of regeneration after *cbp2* RNAi that coincides with the time the animals start dying.

Alternatively, previous studies have demonstrated a role of CBP in cell viability, as suggested by the induction of apoptosis after inhibition of β-catenin/CBP signalling (Kleszcz et al., 2019). In the parasitic worm *S. mansoni* silencing of the Smed-*cbp-2* homologue (called *Sm-cbp1,* Fig. S1) also results in a lethal phenotype, apparently triggered by an increase in cell death (Collins and Collins, 2016). Further experiments are required to characterise the role of *cbp-2* in cell death. In the case of *cbp-3*, after its inhibition, we observed an increased number of *Smedwi-1*+ cells within the blastema, together with an overall lack of differentiation within it. As epidermal progenitors have been shown to be highly migratory (Abnave et al., 2017) further experiments are necessary to discern whether their accumulation within the blastema of *cbp-3(RNAi)* animals is due to a function of *cbp-3* in the migration of such progenitors or a consequence of an overall accumulation of *Smedwi-1*+ neoblasts within it. Finally, our results suggest that *cbp*-3 might be required for the specification of neural, photoreceptor, and protonephridia progenitors but not gut and epidermal progenitors, which appear to require *cbp-3* for their final differentiation.

Given that *cbp* genes may exert their functions via multiple types of

interactions with hundreds of factors, it is difficult to pinpoint the mechanisms underlying the wide variety of phenotypes resulting from *cbp-2* and *cbp-3* silencing in our study. Interestingly, analyses of the predicted interactomes of these 2 proteins revealed putative interactions of CBP-2 and CBP-3 with multiple proteins previously characterised in planarians (Fig. S10). Based on our current vertebrate knowledge some of these interactions would be mediated by the acetylation of partners such as β-CATENIN, RUNX1, SETD1A, and SMAD3, while for other partners such as ETS2, MSX1, NEUREGULIN and P53 other types of interactions would be established. For example, silencing of a planarian ETS transcription factor results in a decrease in body-wall pigmentation (He et al., 2017). As described above, *cbp-3* silencing impairs the differentiation of pigmented cells within blastemas. Silencing of *b-catenin* and *Runx1* has also been linked to impaired neural differentiation during planarian regeneration (Sandmann et al., 2011; Sureda-Gómez et al., 2016; Dong et al., 2018; Zou et al., 2020). Similarly, CBP/p300 interacts with Smad3 and p53 to regulate cell differentiation (Jain et al., 2012; Furumatsu et al., 2005; Martire et al., 2020), and is required for normal epidermal regeneration through interaction with KLF3, among other factors (Jones et al., 2020). Finally, the silencing of the chromatin remodeler *mll1/2* leads to the loss of cilia of the epidermal cells in planarians (Duncan et al., 2016) which opens the door to further analyze its relationship with planarian *cbp* genes which seem also required for cilia differentiation.

In summary, our results suggest that planarian *cbp* genes appear to play a conserved role as key regulators of stem cell maintenance, specification and differentiation (Fig. 7) in agreement with similar results obtained from the laboratory of Dr. Roberts-Galbraith (Stelman et al., 2021). Because post-translational modifications play key roles in the regulation of stem cell proliferation and differentiation in humans and planarians (Strand et al., 2019; Wang et al., 2014), further experiments should investigate which specific functions of *cbp-2* and *cbp-3* may be mediated either by direct acetylation of their partners or by acetylation of histone residues, resulting in chromatin remodelling central to the regulation of gene expression.

4. Materials and methods

4.1. Animals and gene nomenclature

S. mediterranea from the asexual clonal line BCN-10 were used for all experiments. Animals were maintained at 20 °C in 1X PAM water as previously described (Cebrià and Newmark, 2005). Animals were fed twice per week with organic veal liver, and were starved for at least 1 week before experiments. For irradiation experiments, planarians were exposed to 86 Gy (Gy) of γ-irradiation.

4.2. CBPs domain arrangement analyses

cbp genes were identified from the *S. mediterranea* genome (Grohme et al., 2018) and amplified using specific primers (Table S1). Protein domain conservation of *Smed-cbps* (Fig. 1D) was analysed using the SMART (http://smart.embl-heidelberg.de) and Pfam protein domain databases (http://pfam.xfam.org/).

4.3. Sequence and phylogenetic analyses

Protein sequences of CBP/P300 homologues were obtained from NCBI, JGI (https://jgi.doe.gov) and Planmine v3.0 (Rozanski et al., 2019) and aligned using MAFFT with the L–INS–i strategy (Katoh et al., 2019). The conserved aligned region comprising the Bromo, KAT11, ZnF_ZZ and ZnF_TAZ domains was used to reconstruct the phylogenetic tree in Fig. S1A. The aligned full sequence of CBP was used to reconstruct the Platyhelminthes tree in Fig. S1B. . The phylogenetic tree was inferred with the IQ-TREE web server, with default options, including the automatic substitution model selector, the ultrafast bootstrap analysis (1000 replicates) and the single branch test number (1000 replicates) (Minh et al., 2013; Trifinopoulos et al., 2016). The approximate Bayes test option was selected. The phylogenetic tree was visualised using FigTree v1.4.4 (http://tree.bio.ed.ac.uk/software/figtree/).

4.4. RNA interference

Double-stranded RNA (dsRNA) for *Smed-cbp* genes were synthesised as previously described (Sánchez-Alvarado and Newmark, 1999). The injection protocol consisted of 1 round (for *cbp-2*) or 2 rounds (for *cbp-1, -3, -4, -5*), of 3 consecutive days of injections separated by a 4-day interval. A Nanoject II (Drummond Scientific, Broomall, PA, USA) was used to administer 3 injections of 32 nl of dsRNA (1 μg/μl) per day. Control animals were injected with *gfp* dsRNA. In each round, one day after the third day of injection, planarians underwent pre-pharyngeal amputation to induce anterior regeneration. In some experiments, animals were kept intact to analyze the effects of gene silencing on homeostasis.

4.5. Single-cell sequencing (SCS) data

cbp gene expression profiles were obtained from the planaria single-cell database hosted by the Rajewsky lab at the Berlin Institute for Medical Systems Biology of the Max Delbrück Center, Berlin (Plass et al., 2018), the planaria single-cell database hosted by the Sanchez lab at Planosphere website (Zeng et al., 2018) and the Gene Co-expression Counts tool hosted on the PlanNET website (Castillo-Lara and Abril 2018; Castillo-Lara et al., 2020).

4.6. WISH and WFISH

Whole-mount *in situ* hybridisation (WISH) (Currie et al., 2016) and whole-mount fluorescent *in situ* hybridisation (WFISH) (King and Newmark, 2013) were performed as previously described. Riboprobes for *in situ* hybridisation were synthesised using the DIG RNA labelling kit (Sp6/T7, Roche) following the manufacturer's instructions. Samples were mounted in 70% glycerol/PBS solution.

4.7. Immunohistochemistry

Whole-mount immunohistochemistry was performed as previously described (Ross et al., 2015). Treated animals were euthanised by immersion in cold 2% HCl in ultrapure H_2O for 5 min and then washed with PBS-Tx (PBS + 0.3% Triton X-100) at room temperature (RT) for 5 min with agitation. Next, they were placed in a fixative solution (4% formaldehyde in PBS-Tx) for 15 min at RT with agitation and washed twice with PBS-Tx. Subsequently, samples were bleached in 6% H_2O_2 (in PBS-Tx) at RT for 16 h under direct light. The following day, bleached animals were washed with PBS-Tx and incubated for 2 h in 1% blocking solution (1% BSA in PBS-Tx), and then overnight at 4 °C in the primary antibody (diluted in blocking solution). The following primary antibodies were used: anti-phospho-histone3 (PH3, Cell Signalling Technology) to detect mitotic cells which are between the G2 and M phases, diluted 1:300; anti-SYNAPSIN, used as a pan-neural marker (anti--SYNORF1, Developmental Studies Hybridoma Bank), diluted 1:50; anti-VC-1, specific for planarian photosensitive cells (Sakai et al., 2000), diluted 1:15000; anti-SMEDWI-1, specific for neoblasts, diluted 1:1500 (Guo et al., 2006; März et al., 2013); TMUS-13, specific for myosin heavy chain (Cebrià et al., 1997), diluted 1:5; and AA4.3 (Developmental Studies Hybridoma Bank), specific for a-tubulin to visualise the epithelial cilia, diluted 1:20. The following secondary antibodies were used: Alexa-488-conjugated goat anti-mouse (Molecular Probes) for SYNAPSIN, VC1, TMUS-13, and AA4.3, diluted 1:400; and Alexa 568-conjugated goat anti-rabbit (Molecular Probes) for PH3 and SMEDWI-1, diluted 1:1000. Samples were mounted in 70% glycerol/PBS solution. Nuclei were stained with DAPI (1:5000; Sigma-Aldrich) and TO-PRO®-3 (1:3000, Thermo Fisher Scientific, Waltham, MA, USA).

4.8. Microscopy, image acquisition, and image analysis

Live animals were photographed with an sCM EX-3 high end digital microscope camera (DC.3000s, Visual Inspection Technology). WISH, WFISH, and immunostained animals were observed with a Leica MZ16F stereomicroscope. Images were captured with the ProGres C3 camera (Jenoptik) and then processed in Photoshop CS6 for publication. Representative images of WFISH and immunostained animals were captured with confocal laser scanning microscopy (Leica TCS-SPE microscope) and processed in ImageJ1.51d and Photoshop CS6 for publication.

4.9. Quantitative real time PCR (qPCR)

qPCR was performed with 3 technical and biological replicates following MIQE guidelines (Bustin et al., 2009). Following RNAi injections, total RNA was isolated from a pool of 5 treated planarians per condition by homogenisation in TRIzol Reagent (Invitrogen). The housekeeping gene *ura4* was used to normalise expression levels.

4.10. Statistical analysis

All comparisons were performed using the unpaired Student's t-test, after first confirming data normality and homogeneity using the Shapiro-Wilk test.

Funding

M.D.M. has received funding from the postdoctoral fellowship programme Beatriu de Pinós, funded by the Secretary of Universities and Research (Government of Catalonia) and by the European Union Horizon 2020 research and innovation programme under Marie Sklodowska-Curie grant agreement No. 801370. F.C. was supported by grants BFU 2015-65704-P and PGC 2018-100747-B-100 from the Ministerio de Ciencia, Innovación y Universidades, Spain, and grant 2017 SGR 1455 from AGAUR, Generalitat de Catalunya.

Author contributions

Conceived and designed the experiments, SF, MDM, FC; performed the experiments, SF, SC, CV, MDM, JG, JM; analysed the data, SF, SC, CV, JG, MDM, JM, FC, RR, TS, KB; wrote the paper, SF, MDM, FC.

Acknowledgments

We thank all members of the E. Saló and T. Adell laboratory for discussions and H. Orii and Prof. K. Watanabe for providing anti-VC-1. Monoclonal anti-SYNORF1 antibody was obtained from the Developmental Studies Hybridoma Bank, developed under the auspices of the National Institute of Child Health and Human Development and maintained by the Department of Biological Sciences, University of Iowa, Iowa City, IA, USA. We thank Owen Howard for advice on English style.

Appendix A. Supplementary data

Supplementary data to this article can be found online at https://doi.org/10.1016/j.ydbio.2021.02.008.

References

Abnave, P., Aboukhatwa, E., Kosaka, N., Thompson, J., Hill, M.A., Aboobaker, A.A., 2017. Epithelial-mesenchymal transition transcription factors control pluripotent adult stem cell migration *in vivo* in planarians. Development 144, 3440–3453. https://doi.org/10.1242/dev.154971.

Avgustinova, A., Benitah, S.A., 2016. Epigenetic control of adult stem cell function. Nat. Rev. Mol. Cell Biol. 17 (10), 643–658. https://doi.org/10.1038/nrm.2016.76.

Baguñà, J., Saló, E., Collet, J., Auladell, M.C., Ribas, M., 1988. Cellular, molecular and genetic approaches to regeneration and pattern formation in planarians. Fortschr. Zool. 36, 65–78.

Baguñà, J., 2012. The planarian neoblast: the rambling history of its origin and some current black boxes. Int. J. Dev. Biol. 56 (1–3), 19–37. https://doi.org/10.1387/ijdb.113463jb.

Barberán, S., Fraguas, S., Cebrià, F., 2016. The EGFR signaling pathway controls gut progenitor differentiation during planarian regeneration and homeostasis. Development 143 (12), 2089–2102. https://doi.org/10.1242/dev.131995.

Bedford, D.C., Kasper, L.H., Fukuyama, T., Brindle, P.K., 2010. Target gene context influences the transcriptional requirement for the KAT3 family of CBP and p300 histone acetyltransferases. Epigenetics 5 (1), 9–15. https://doi.org/10.4161/epi.5.1.10449.

Bonuccelli, L., Rossi, L., Lena, A., Scarcelli, V., Rainaldi, G., Evangelista, M., Iacopetti, P., Gremigni, V., Salvetti, A., 2010. An RbAp48-like gene regulates adult stem cells in planarians. J. Cell Sci. 123 (Pt 5), 690–698. https://doi.org/10.1242/jcs.053900.

Brai, E., Marathe, S., Astori, S., Fredj, N.B., Perry, E., Lamy, C., Scotti, A., Alberi, L., 2015. Notch1 regulates hippocampal plasticity through interaction with the reelin pathway, glutamatergic transmission and CREB signaling. Front. Cell. Neurosci. 9, 447. https://doi.org/10.3389/fncel.2015.00447.

Bustin, S.A., Benes, V., Garson, J.A., Hellemans, J., Huggett, J., Kubista, M., Mueller, R., Nolan, T., Pfaffl, M.W., Shipley, G.L., Vandesompele, J., Wittwer, C.T., 2009. The MIQE guidelines: minimum information for publication of quantitative real-time PCR experiments. Clin. Chem. 5 (4), 611–622. https://doi.org/10.1373/clinchem.2008.112797.

Castillo-Lara, S., Abril, J.F., 2018. PlanNET: homology-based predicted interactome for multiple planarian transcriptomes. Bioinformatics 34 (6), 1016–1023. https://doi.org/10.1093/bioinformatics/btx738.

Castillo-Lara, S., Pascual-Carreras, E., Abril, J.F., 2020. PlanExp: intuitive integration of complex RNA-seq datasets with planarian omics resources. Bioinformatics 36 (6), 1889–1895. https://doi.org/10.1093/bioinformatics/btz802.

Cebrià, F., Vispo, M., Newmark, P., Bueno, D., Romero, R., 1997. Myocyte differentiation and body wall muscle regeneration in the planarian Girardia tigrina. Dev. Gene. Evol. 207 (5), 306–316. https://doi.org/10.1007/s004270050118.

Cebrià, F., Newmark, P.A., 2005. Planarian homologs of netrin and netrin receptor are required for proper regeneration of the central nervous system and the maintenance of nervous system architecture. Development 132 (16), 3691–3703. https://doi.org/10.1242/dev.01941.

Chan, H.M., La Thangue, N.B., 2001. p300/CBP proteins: HATs for transcriptional bridges and scaffolds. J. Cell Sci. 114 (Pt 13), 2363–2373.

Chandebois, R., 1980. Cell sociology and the problem of automation in the development of pluricellular animals. Acta Biotheor. 29 (1), 1–35. https://doi.org/10.1007/BF00045880.

Cheng, L.C., Tu, K.C., Seidel, C.W., Robb, S.M.C., Guo, F., Sánchez Alvarado, A., 2018. Cellular, ultrastructural and molecular analyses of epidermal cell development in the planarian Schmidtea mediterranea. Dev. Biol. 433 (2), 357–373. https://doi.org/10.1016/j.ydbio.2017.08.030.

Chrivia, J.C., Kwok, R.P., Lamb, N., Hagiwara, M., Montminy, M.R., Goodman, R.H., 1993. Phosphorylated CREB binds specifically to the nuclear protein CBP. Nature 365 (6449), 855–859. https://doi.org/10.1038/365855a0.

Collins, J.N., Collins 3rd, J.J., 2016. Tissue degeneration following loss of schistosoma mansoni cbp1 is associated with increased stem cell proliferation and parasite death in vivo. PLoS Pathog. 12 (11), e1005963 https://doi.org/10.1371/journal.ppat.1005963.

Cowles, M.W., Brown, D.D., Nisperos, S.V., Stanley, B.N., Pearson, B.J., Zayas, R.M., 2013. Genome-wide analysis of the bHLH gene family in planarians identifies factors required for adult neurogenesis and neuronal regeneration. Development 140 (23), 4691–4702. https://doi.org/10.1242/dev.098616.

Currie, K.W., Brown, D.D., Zhu, S., Xu, C., Voisin, V., Bader, G.D., Pearson, B.J., 2016. HOX gene complement and expression in the planarian Schmidtea mediterranea. EvoDevo 7, 7. https://doi.org/10.1186/s13227-016-0044-8.

Dancy, B.M., Cole, P.A., 2015. Protein lysine acetylation by p300/CBP. Chem. Rev. 115 (6), 2419–2452. https://doi.org/10.1021/cr500452k.

Dattani, A., Kao, D., Mihaylova, Y., Abnave, P., Hughes, S., Lai, A., Sahu, S., Aboobaker, A.A., 2018. Epigenetic analyses of planarian stem cells demonstrate conservation of bivalent histone modifications in animal stem cells. Genome Res. 28 (10), 1543–1554. https://doi.org/10.1101/gr.239848.118.

Dattani, A., Sridhar, D., Aziz Aboobaker, A.A., 2019. Planarian flatworms as a new model system for understanding the epigenetic regulation of stem cell pluripotency and differentiation. Semin. Cell Dev. Biol. 87, 79–94. https://doi.org/10.1016/j.semcdb.2018.04.007.

Dong, Z., Yang, Y., Chen, G., Liu, D., 2018. Identification of runt family genes involved in planarian regeneration and tissue homeostasis. Gene Expr. Patterns 29, 24–31. https://doi.org/10.1016/j.gep.2018.04.006.

Duncan, E.M., Chitsazan, A.D., Seidel, C.W., Sánchez Alvarado, A.S., 2016. Set1 and MLL1/2 target distinct sets of functionally different genomic loci in vivo. Cell Rep. 17 (3), 930. https://doi.org/10.1016/j.celrep.2016.09.071.

Dutto, I., Scalera, C., Prosperi, E., 2018. CREBBP and p300 lysine acetyl transferases in the DNA damage response. Cell. Mol. Life Sci. 75 (8), 1325–1338. https://doi.org/10.1007/s00018-017-2717-4.

Esvald, E.E., Tuvikene, J., Sirp, A., Patil, S., Bramham, C.R., Timmusk, T., 2020. CREB family transcription factors are major mediators of BDNF transcriptional autoregulation in cortical neurons. J. Neurosci. 40 (7), 1405–1426. https://doi.org/10.1523/jneurosci.0367-19.2019.

Fincher, C.T., Wurtzel, O., de Hoog, T., Kravarik, K.M., Reddien, P.W., 2018. Cell type transcriptome atlas for the planarian Schmidtea mediterranea. Science 360 (6391). https://doi.org/10.1126/science.aaq1736.

Furumatsu, T., Tsuda, M., Taniguchi, N., Tajima, Y., Asahara, H., 2005. Smad3 induces chondrogenesis through the activation of SOX9 via CREB-binding protein/p300 recruitment. J. Biol. Chem. 280 (9), 8343–8350. https://doi.org/10.1074/jbc.M413913200.

Gavino, M.A., Reddien, P.W., 2011. A Bmp/Admp regulatory circuit controls maintenance and regeneration of dorsal-ventral polarity in planarians. Curr. Biol. 21 (4), 294–299. https://doi.org/10.1016/j.cub.2011.01.017.

Giordano, A., Avantaggiati, M.L., 1999. p300 and CBP: partners for life and death. J. Cell. Physiol. 181 (2), 218–230. https://doi.org/10.1002/(sici)1097-4652(199911)181:2<218::Aid-jcp4>3.0.Co;2-5.

Godini, R., Lafta, H.Y., Fallahi, H., 2018. Epigenetic modifications in the embryonic and induced pluripotent stem cells. Gene Expr. Patterns 29, 1–9. https://doi.org/10.1016/j.gep.2018.04.001.

Goodman, R.H., Smolik, S., 2000. CBP/p300 in cell growth, transformation, and development. Genes Dev. 14 (13), 1553–1577.

Grohme, M.A., Schloissnig, S., Rozanski, A., Pippel, M., Young, G.R., Winkler, S., Brandl, H., Henry, I., Dahl, A., Powell, S., Hiller, M., Myers, E., Rink, J.C., 2018. The genome of Schmidtea mediterranea and the evolution of core cellular mechanisms. Nature 554 (7690), 56–61. https://doi.org/10.1038/nature25473.

Guo, L., Zhang, S., Rubinstein, B., Ross, E., Sánchez Alvarado, A., 2006. Widespread maintenance of genome heterozygosity in Schmidtea mediterranea. Nat Ecol Evol 1 (1), 19. https://doi.org/10.1038/s41559-016-0019.

He, X., Lindsay-Mosher, N., Li, Y., Molinaro, A.M., Pellettieri, J., Pearson, B.J., 2017. FOX and ETS family transcription factors regulate the pigment cell lineage in planarians. Development 144 (24), 4540–4551. https://doi.org/10.1242/dev.156349.

Hardingham, G.E., Arnold, F.J., Bading, H., 2001. Nuclear calcium signaling controls CREB-mediated gene expression triggered by synaptic activity. Nat. Neurosci. 4 (3), 261–267. https://doi.org/10.1038/85109.

Henderson, J.M., Nisperos, S.V., Weeks, J., Ghulam, M., Marín, I., Zayas, R.M., 2015. Identification of HECT E3 ubiquitin ligase family genes involved in stem cell regulation and regeneration in planarians. Dev. Biol. 404 (2), 21–34. https://doi.org/10.1016/j.ydbio.2015.04.021.

Holmqvist, P.H., Mannervik, M., 2013. Genomic occupancy of the transcriptional co-activators p300 and CBP. Transcription 4 (1), 18–23. https://doi.org/10.4161/trns.22601.

Hyman, L.H., 1951. The Invertebrates : Platyhelminthes and Rhynchocoela, the Acoelomate Bilateria, vol. 2. McGraw-Hill Book Company Inc., New York, p. 550 vii +.

Iglesias, M., Gomez-Skarmeta, J.L., Salo, E., Adell, T., 2008. Silencing of Smed-betacatenin1 generates radial-like hypercephalized planarians. Development 135 (7), 1215–1221. https://doi.org/10.1242/dev.020289.

Jain, A.K., Allton, K., Iacovino, M., Mahen, E., Milczarek, R.J., Zwaka, T.P., Kyba, M., Barton, M.C., 2012. p53 regulates cell cycle and microRNAs to promote differentiation of human embryonic stem cells. PLoS Biol. 10 (2), e1001268 https://doi.org/10.1371/journal.pbio.1001268.

Jones, J., Chen, Y., Tiwari, M., Li, J., Ling, J., Sen, G.L., 2020. KLF3 mediates epidermal differentiation through the epigenomic writer CBP. Science 23 (7), 101320. https://doi.org/10.1016/j.isci.2020.101320.

Kato, Y., Shi, Y., He, X., 1999. Neuralization of the Xenopus embryo by inhibition of p300/CREB-binding protein function. J. Neurosci. 19 (21), 9364–9373. https://doi.org/10.1523/jneurosci.19-21-09364.1999.

Katoh, K., Rozewicki, J., Yamada, K.D., 2019. MAFFT online service: multiple sequence alignment, interactive sequence choice and visualization. Briefings Bioinf. 20 (4), 1160–1166. https://doi.org/10.1093/bib/bbx108. Jul 19.

King, R.S., Newmark, P.A., 2013. In situ hybridization protocol for enhanced detection of gene expression in the planarian Schmidtea mediterranea. BMC Dev. Biol. 13, 8. https://doi.org/10.1186/1471-213x-13-8.

Kleszcz, R., Szymańska, A., Krajka-Kuźniak, V., Baer-Dubowska, W., Paluszczak, J., 2019. Inhibition of CBP/β-catenin and porcupine attenuates Wnt signaling and induces apoptosis in head and neck carcinoma cells. Cell. Oncol. 42 (4), 505–520. https://doi.org/10.1007/s13402-019-00440-4.

Lapan, S.W., Reddien, P.W., 2012. Transcriptome analysis of the planarian eye identifies ovo as a specific regulator of eye regeneration. Cell Rep. 2 (2), 294–307. https://doi.org/10.1016/j.celrep.2012.06.018.

Lundblad, J.R., Kwok, R.P., Laurance, M.E., Harter, M.L., Goodman, R.H., 1995. Adenoviral E1A-associated protein p300 as a functional homologue of the transcriptional co-activator CBP. Nature 374 (6517), 85–88. https://doi.org/10.1038/374085a0.

Manegold, P., Lai, K.K.Y., Wu, Y., Teo, J.L., Lenz, H.J., Genyk, Y.S., Pandol, S.J., Wu, K., Lin, D.P., Chen, Y., Nguyen, C., Zhao, Y., Kahn, M., 2018. Differentiation therapy targeting the β-catenin/CBP interaction in pancreatic cancer. Cancers 10 (4). https://doi.org/10.3390/cancers10040095.

Martire, S., Nguyen, J., Sundaresan, A., Banaszynski, L.A., 2020. Differential contribution of p300 and CBP to regulatory element acetylation in mESCs. BMC Mol Cell Biol 21 (1), 55. https://doi.org/10.1186/s12860-020-00296-9.

März, M., Seebeck, F., Bartscherer, K., 2013. A Pitx transcription factor controls the establishment and maintenance of the serotonergic lineage in planarians. Development 140 (22), 4499–4509. https://doi.org/10.1242/dev.100081.

Mayr, B., Montminy, M., 2001. Transcriptional regulation by the phosphorylation-dependent factor CREB. Nat. Rev. Mol. Cell Biol. 2 (8), 599–609. https://doi.org/10.1038/35085068.

Mihaylova, Y., Abnave, P., Kao, D., Hughes, S., Lai, A., Jaber-Hijazi, F., Kosaka, N., Aboobaker, A.A., 2018. Conservation of epigenetic regulation by the MLL3/4 tumour suppressor in planarian pluripotent stem cells. Nat. Commun. 9 (1), 3633. https://doi.org/10.1038/s41467-018-06092-6.

Minh, B.Q., Nguyen, M.A.T., von Haeseler, A., 2013. Ultrafast approximation for phylogenetic bootstrap. Mol. Biol. Evol. 30, 1188–1195.

Molina, M.D., Salo, E., Cebria, F., 2007. The BMP pathway is essential for re-specification and maintenance of the dorsoventral axis in regenerating and intact planarians. Dev. Biol. 311 (1), 79–94. https://doi.org/10.1016/j.ydbio.2007.08.019.

Molina, M.D., Saló, E., Cebrià, F., 2009. Expression pattern of the expanded noggin gene family in the planarian Schmidtea mediterranea. Gene Expr. Patterns 9 (4), 246–253. https://doi.org/10.1016/j.gep.2008.12.008.

Molina, M.D., Neto, A., Maeso, I., Gómez-Skarmeta, J.L., Saló, E., Cebrià, F., 2011. Noggin and noggin-like genes control dorsoventral axis regeneration in planarians. Curr. Biol. 21 (4), 300–305. https://doi.org/10.1016/j.cub.2011.01.016.

Owlarn, S., Klenner, F., Schmidt, D., Rabert, F., Tomasso, A., Reuter, H., Mulaw, M.A., Moritz, S., Gentile, L., Weidinger, G., Bartscherer, K., 2017. Generic wound signals initiate regeneration in missing-tissue contexts. Nat. Commun. 8 (1), 2282. https://doi.org/10.1038/s41467-017-02338-x.

Pellettieri, J., Fitzgerald, P., Watanabe, S., Mancuso, J., Green, D.R., Sánchez Alvarado, A., 2010. Cell death and tissue remodeling in planarian regeneration. Dev. Biol. 338 (1), 76–85. https://doi.org/10.1016/j.ydbio.2009.09.015.

Plass, M., Solana, J., Wolf, F.A., Ayoub, S., Misios, A., Glažar, P., Obermayer, B., Theis, F.J., Kocks, C., Rajewsky, N., 2018. Cell type atlas and lineage tree of a whole complex animal by single-cell transcriptomics. Science 360 (6391). https://doi.org/10.1126/science.aaq1723.

Reddien, P.W., 2013. Specialized progenitors and regeneration. Development 140 (5), 951–957. https://doi.org/10.1242/dev.080499.

Reddien, P.W., 2018. The cellular and molecular basis for planarian regeneration. Cell 175 (2), 327–345. https://doi.org/10.1016/j.cell.2018.09.021.

Rink, J.C., 2013. Stem cell systems and regeneration in planaria. Dev. Gene. Evol. 223 (1–2), 67–84. https://doi.org/10.1007/s00427-012-0426-4.

Robb, S.M., Sánchez Alvarado, A., 2014. Histone modifications and regeneration in the planarian Schmidtea mediterranea. Curr. Top. Dev. Biol. 108, 71–93. https://doi.org/10.1016/b978-0-12-391498-9.00004-8.

Rompolas, P., Patel-King, R.S., King, S.M., 2010. An outer arm Dynein conformational switch is required for metachronal synchrony of motile cilia in planaria. Mol. Biol. Cell 21 (21), 3669–3679. https://doi.org/10.1091/mbc.E10-04-0373.

Ross, K.G., Omuro, K.C., Taylor, M.R., Munday, R.K., Hubert, A., King, R.S., Zayas, R.M., 2015. Novel monoclonal antibodies to study tissue regeneration in planarians. BMC Dev. Biol. 15, 2. https://doi.org/10.1186/s12861-014-0050-9.

Ross, K.G., Molinaro, A.M., Romero, C., Dockter, B., Cable, K.L., González, K., Zhang, S., Collins, E.S., Pearson, B.J., Zayas, R.M., 2018. SoxB1 activity regulates sensory neuron regeneration, maintenance, and function in planarians. Dev. Cell 47, 331–347. https://doi.org/10.1016/j.devcel.2018.10.014.

Rozanski, A., Moon, H., Brandl, H., Martín-Durán, J.M., Grohme, M.A., Hüttner, K., Bartscherer, K., Henry, I., Rink, J.C., 2019. PlanMine 3.0-improvements to a mineable resource of flatworm biology and biodiversity. Nucleic Acids Res. 47 (D1), D812–d820. https://doi.org/10.1093/nar/gky1070.

Sakai, F., Agata, K., Orii, H., Watanabe, K., 2000. Organization and regeneration ability of spontaneous supernumerary eyes in planarians -eye regeneration field and pathway selection by optic nerves-. Zool. Sci. 17 (3), 375–381. https://doi.org/10.2108/jsz.17.375.

Salo, E., Baguñá, J., 1984. Regeneration and pattern formation in planarians. I. The pattern of mitosis in anterior and posterior regeneration in Dugesia (G) tigrina, and a new proposal for blastema formation. J. Embryol. Exp. Morphol. 83, 63–80.

Sánchez Alvarado, A., Newmark, P.A., 1999. Double-stranded RNA specifically disrupts gene expression during planarian regeneration. Proc. Natl. Acad. Sci. U. S. A. 96 (9), 5049–5054. https://doi.org/10.1073/pnas.96.9.5049.

Sandmann, T., Vogg, M.C., Owlarn, S., Boutros, M., Bartscherer, K., 2011. The head-regeneration transcriptome of the planarian Schmidtea mediterranea. Genome Biol. 12 (8), R76. https://doi.org/10.1186/gb-2011-12-8-r76.

Scimone, M.L., Meisel, J., Reddien, P.W., 2010. The Mi-2-like Smed-CHD4 gene is required for stem cell differentiation in the planarian Schmidtea mediterranea. Development 137 (8), 1231–1241. https://doi.org/10.1242/dev.042051.

Scimone, M.L., Srivastava, M., Bell, G.W., Reddien, P.W., 2011. A regulatory program for excretory system regeneration in planarians. Development 138 (20), 4387–4398. https://doi.org/10.1242/dev.068098.

Scimone, M.L., Kravarik, K.M., Lapan, S.W., Reddien, P.W., 2014. Neoblast specialization in regeneration of the planarian Schmidtea mediterranea. Stem Cell Reports 3 (2), 339–352. https://doi.org/10.1016/j.stemcr.2014.06.001.

Scimone, M.L., Atabay, K.D., Fincher, C.T., Bonneau, A.R., Li, D.J., Reddien, P.W., 2020. Muscle and neuronal guidepost-like cells facilitate planarian visual system regeneration. Science 368 (6498), eaba3203. https://doi.org/10.1126/science.aba3203.

Shaywitz, A.J., Greenberg, M.E., 1999. CREB: a stimulus-induced transcription factor activated by a diverse array of extracellular signals. Annu. Rev. Biochem. 68, 821–861. https://doi.org/10.1146/annurev.biochem.68.1.821.

Stelman, C.R., Smith, B.M., Chandra, B., Roberts-Galbraith, R.H., 2021. CBP/p300 homologs CBP2 and CBP3 play distinct roles in planarian stem cell function. Dev. Biol. https://doi.org/10.1016/j.ydbio.2021.02.004 (in press).

Strand, N.S., Allen, J.M., Zayas, R.M., 2019. Post-translational regulation of planarian regeneration. Semin. Cell Dev. Biol. 87, 58–68. https://doi.org/10.1016/j.semcdb.2018.04.009.

Su, H., Sureda-Gomez, M., Rabaneda-Lombarte, N., Gelabert, M., Xie, J., Wu, W., Adell, T., 2017. A C-terminally truncated form of β-catenin acts as a novel regulator of Wnt/β-catenin signaling in planarians. PLoS Genet. 13 (10), e1007030 https://doi.org/10.1371/journal.pgen.1007030.

Sureda-Gómez, M., Martín-Durán, J.M., Adell, T., 2016. Localization of planarian β-CATENIN-1 reveals multiple roles during anterior-posterior regeneration and organogenesis. Development 143 (22), 4149–4160. https://doi.org/10.1242/dev.135152.

Thiruvalluvan, M., Barghouth, P.G., Tsur, A., Broday, L., Oviedo, N.J., 2018. SUMOylation controls stem cell proliferation and regional cell death through Hedgehog signaling in planarians. Cell. Mol. Life Sci. 75 (7), 1285–1301. https://doi.org/10.1007/s00018-017-2697-4.

Thomas, P.D., Kahn, M., 2016. Kat3 coactivators in somatic stem cells and cancer stem cells: biological roles, evolution, and pharmacologic manipulation. Cell Biol. Toxicol. 32 (1), 61–81. https://doi.org/10.1007/s10565-016-9318-0.

Trifinopoulos, J., Nguyen, L.T., von Haeseler, A., Minh, B.Q., 2016. W-IQ-TREE: a fast online phylogenetic tool for maximum likelihood analysis. Nucleic Acids Res. 44 (W1), W232–W235. https://doi.org/10.1093/nar/gkw256.

Tu KC, Cheng LC, T K Vu H, Lange JJ, McKinney SA, Seidel CW, Sánchez Alvarado A.Elife. 2015. Egr-5 is a post-mitotic regulator of planarian epidermal differentiation. Oct 12; 4:e10501. https://doi.org/10.7554/eLife.10501.

van Wolfswinkel, J.C., Wagner, D.E., Reddien, P.W., 2014. Single-cell analysis reveals functionally distinct classes within the planarian stem cell compartment. Cell Stem Cell 15 (3), 326–339. https://doi.org/10.1016/j.stem.2014.06.007.

Vásquez-Doorman, C., Petersen, C.P., 2016. The NuRD complex component p66 suppresses photoreceptor neuron regeneration in planarians. Regeneration (Oxf) 3 (3), 168–178. https://doi.org/10.1002/reg2.58.

Voss, A.K., Thomas, T., 2018. Histone lysine and genomic targets of histone acetyltransferases in mammals. Bioessays 40 (10), e1800078. https://doi.org/10.1002/bies.201800078.

Wagner, D.E., Wang, I.E., Reddien, P.W., 2011. Clonogenic neoblasts are pluripotent adult stem cells that underlie planarian regeneration. Science 332 (6031), 811–816. https://doi.org/10.1126/science.1203983.

Wang, F., Marshall, C.B., Ikura, M., 2013. Transcriptional/epigenetic regulator CBP/p300 in tumorigenesis: structural and functional versatility in target recognition. Cell. Mol. Life Sci. 70 (21), 3989–4008. https://doi.org/10.1007/s00018-012-1254-4.

Wang, Y.C., Peterson, S.E., Loring, J.F., 2014. Protein post-translational modifications and regulation of pluripotency in human stem cells. Cell Res. 24 (2), 143–160. https://doi.org/10.1038/cr.2013.151.

Wen, A.Y., Sakamoto, K.M., Miller, L.S., 2010. The role of the transcription factor CREB in immune function. J. Immunol. 185 (11), 6413–6419. https://doi.org/10.4049/jimmunol.1001829.

Wenemoser, D., Lapan, S.W., Wilkinson, A.W., Bell, G. W. a, Reddien, P.W., 2012. A molecular wound response program associated with regeneration initiation in planarians. Genes Dev. 26 (9), 988–1002. https://doi.org/10.1101/gad.187377.112.

Wenemoser, D., Reddien, P.W., 2010. Planarian regeneration involves distinct stem cell responses to wounds and tissue absence. Dev. Biol. 344 (2), 979–991. https://doi.org/10.1016/j.ydbio.2010.06.017.

Wurtzel, O., Oderberg, I.M., Reddien, P.W., 2017. Planarian epidermal stem cells respond to positional cues to promote cell-type diversity. Dev. Cell 40 (5), 491–504. https://doi.org/10.1016/j.devcel.2017.02.008 e495.

Yuan, L.W., Giordano, A., 2002. Acetyltransferase machinery conserved in p300/CBP-family proteins. Oncogene 21 (14), 2253–2260. https://doi.org/10.1038/sj.onc.1205283.

Zeng, A., Li, H., Guo, L., Gao, X., McKinney, S., Wang, Y., Yu, Z., Park, J., Semerad, C., Ross, E., Cheng, L.C., Davies, E., Lei, K., Wang, W., Perera, A., Hall, K., Peak, A., Box, A., Sánchez Alvarado, A., 2018. Prospectively isolated Tetraspanin(+) neoblasts are adult pluripotent stem cells underlying planaria regeneration. Cell 173 (7), 1593–1608. https://doi.org/10.1016/j.cell.2018.05.006 e20.

Zou, L., Li, H., Han, X., Qin, J., Song, G., 2020. Runx1t1 promotes the neuronal differentiation in rat hippocampus. Stem Cell Res. Ther. 11 (1), 160. https://doi.org/10.1186/s13287-020-01667-x.

Zhu, S.J., Hallows, S.E., Currie, K.W., Xu, C., Pearson, B.J., 2015. A mex3 homolog is required for differentiation during planarian stem cell lineage development. Elife 4. https://doi.org/10.7554/eLife.07025.

Zhu, S.L., Pearson, B.J., 2016. (Neo)blast from the past: new insights into planarian stem cell lineages. Curr. Opin. Genet. Dev. 40, 74–80. https://doi.org/10.1016/j.gde.2016.06.007.

Zhu, S.J., Pearson, B.J., 2018. Smed-myb-1 specifies early temporal identity during planarian epidermal differentiation. Cell Rep. 25 (1), 38–46. https://doi.org/10.1016/j.celrep.2018.09.011 e33.